Joint Defra/EA Flood and Coastal Erosion Risk Management R&D Programme

Performance and Reliability of Flood and Coastal Defences

R&D Technical Report FD2318/TR 2
(Final Draft)

Produced: October 2005

Author(s): Foekje Buijs
Jonathan Simm
Michael Wallis
Paul Sayers

Statement of use

Dissemination status
Publicly available/Restricted

Keywords:
Maximum of 10

Research contractor:
HR Wallingford Ltd, Howbery Park, Wallingford, Oxon, OX11 8BA.
+44 (0)1491 835381

Defra project officer:
Ian Meadowcroft, Reading

Publishing organisation
Department for Environment, Food and Rural Affairs
Flood Management Division,
Ergon House,
Horseferry Road
London SW1P 2AL

Tel: 020 7238 3000 Fax: 020 7238 6187

www.defra.gov.uk/environ/fcd

Published by the Department for Environment, Food and Rural Affairs. Printed in the UK, (*insert month, year*) on recycled material containing 80% post-consumer waste and 20% chlorine-free virgin pulp.

PB No. *xxxxx* ISBN: *xxxxxx*

Preface

This document reports the findings of research into the "Performance and reliability of flood and coastal defences"- Phase I" - Project FD2318 in the Risk Theme of the Joint Defra/EA Flood and Coastal Erosion Risk Management R&D Programme. This project has explored ways to assess the performance and reliability of flood and coastal defences in order to make better assessments of risk. It directly supports Defra and Environment Agency policies, strategies and new decision-making tools for flood and coastal risk management. In particular:

- it provides information to assess the effectiveness of flood defences in reducing risk
- it provides information to support decision-making on how to manage the performance of flood defences
- it provides methods to help to assess flood and erosion risk including performance of defences under extreme loads.

The project reviewed a range of methods for assessing the reliability of different types of defences, including their deterioration in time. It then focussed on developing practical methods for assessing reliability[1] using 'fragility curves'. A fragility curve summarises information about the probability of failure of an engineering system such as a flood defence, in response to a specific range of loads (eg high water levels or waves). This report presents the main findings of the project including the methodology developed to construct fragility curves.

This report is aimed at those carrying out, or with an interest in, flood and coastal risk assessment. It describes the scientific and practical basis for fragility curves, and their role in the risk and performance based management framework (Ref: FD2318/TR). The report is intended to inform and assist those involved with managing flood and coastal defences, and assessing risk associated with flood defence structures and systems. FD2318/TR2 compliments this report by providing a more in-depth technical background including the mathematical equations of failure processes that were used for fragility calculation.

[1] Reliability is the complement of failure probability. For example a defence may have a reliability of 0.99 or a failure probability of 0.01 per year - the meaning is the same

Executive summary

This report summarises key findings of R&D project FD2318, 'Performance and Reliability of Flood and Coastal Defences'. The objectives of the overall study were:

- To explore the available approaches to characterising the reliability of flood and coastal defences
- To develop scientifically justified fragility curves capturing information about the performance of structures under a variety of loading conditions.
- To provide clear guidance on developing and using fragility curves for reliability analysis of linear defences.

This project has investigated and considered how the concept of fragility can be practically applied to the assessment of flood and coastal defence assets. It looked at how other industries use 'fragility' and then developed a technical basis for its application in flood and coastal defence management.

The concept of fragility expresses the probability of failure given a range of loading conditions and summarises the information about the reliability of a flood or coastal defence. Useful by-products are knowledge about the most prominent failure modes (in detailed level risk assessments) and the characteristics of the structure that contribute most to failure of the defence. Moreover, the concept of fragility allows the combination of conditional probabilities of failure with complex consequence of failure scenarios.

The report aims to assist:

- Those involved with managing flood and coastal defences, and assessing risk associated with flood defence structures and systems.
- The further development of Defra and Environment Agency policies, strategies and new decision-making tools for flood and coastal risk management.

Please note that this is a research and development (R&D) output and no part of this report constitutes formal Agency or Defra policy or process.

This report is composed of two volumes. Volume one (TR 1) states the conceptual reasoning behind the application of the fragility curve method which is discussed. A step by step guide to the construction of fragility curves is provided along with additional guidance and includes generic fragility curves. Volume two (TR 2) provides more in-depth technical treatment including the reliability functions that have been used. Chapter one introduces the RASP (Risk Assessment of flood and coastal defence for Strategic Planning) defence classifications and the approach to fragility used for National Flood Risk Assessment (NaFRA). Chapter two shows how fragility curves were created for the High Level Plus method of flood risk assessment and Chapter 3 introduces a more detailed approach to capture indicative failure modes in fragility.

Acknowledgements

This Defra-funded project FD2318 was commissioned under the Risk Evaluation and Understanding of Uncertainty Theme of the Joint Defra / Environment Agency Flood and Coastal Defence R&D programme. This report was prepared by Foekje Buijs during her research based at HR Wallingford and Silvia Segura Domínguez, Paul Sayers, Jonathan Simm and Michael Wallis of HR Wallingford, and supported by Steve Oldfield of RMC Consultants. Research contributors included Fola Ogunyoye (failure and deterioration indicators), Philip Smith (geotechnical issues) and Jaap-Jeroen Flikweert (international review and failure case studies) of Royal Haskoning, and Prof. Mark Dyer (geotechnical failure processes) of the University of Strathclyde. The Project Director was Colin Fenn of HR Wallingford. The client project officer was Ian Meadowcroft.

Contents

Tables

Figures

Appendices

1. Introduction

This part of the report, 'TR2', describes fragility curves for National Flood Risk Assessment (NaFRA) and for intermediate and detailed levels of risk assessment. It also provides the technical detail and demonstrates the approach used to establish the indicative failure modes for a range of coastal and fluvial defence types.

In RASP methodology (HR Wallingford, 2004), flood defences are classified into seven major types as shown by the third layer of the hierarchy in Figure 1 below.

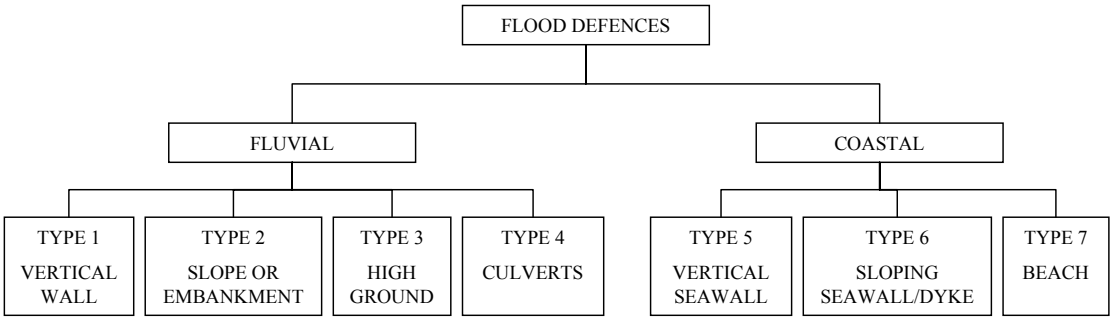

Figure 1 RASP classification of defences

As mentioned in the Literature Review report of "Performance and Reliability of Flood and Coastal defences" project, this classification all together with the definitions for coastal defences lead to the identification of the following main linear defence types:

- Embankment or sloping seawall
- Slope protection against coastal erosion
- Vertical wall structures (e.g. sheet piles, concrete slabs, masonry walls)
- Beaches:
  - Dunes
  - Shingle beaches

Using the above classification, the typical failure and deterioration modes determined from the literature review were summarised as shown in Table 1 of the "Review of Flood and Coastal Defence Failure and Failure Processes" report.

A consultation process involving flood and coastal defence practitioners was carried out to:

- assess the use of this classification of defences,
- test the failure and deterioration modes identified within the literature review with what is observed in practice, and
- identify the key failure modes.

The information obtained from the consultation on the primary classification and failure and deterioration modes for flood defences and coast protection structures was reviewed. A revised table showing how some of the suggestions may be incorporated is shown in Table 1 of the "Review of Flood and Coastal Defence Failure and Failure Processes" report. The classification and list of failure modes are not exhaustive as particular defences such as point structures (gates, sluices, pumps etc) have been omitted and considered separately. The key failure modes identified from the consultation are summarised in Table 1 below.

Table 1 Key Failure Modes identified from the consultation

Flood and coastal defence type		Key Failure Modes
Embankment / sloping seawall		• Erosion of crest and inside face leading to breach following overtopping (possibly induced by settlement) • Piping, excessive seepage, breach or collapse following deterioration due to vermin infestation • Breach following failure of foreign objects or weak spots caused by their presence
Slope protection against erosion		• Structural failure following vandalism • Toe erosion/foundation failure • Slip failure due to instability or foundation failure • Failure of slope drainage • Damage by boats and barges • Structural failure of inflexibility of rigid revetments placed on dynamic watercourses/coastlines
Vertical wall structures		• Overtopping • Toe erosion • Failure of structural members (e.g. tie-rod or anchorage system) • Structural failure due to wash out of fill following joint failure • Structural failure following abrasion or corrosion
Beaches	Sand / Shingle Beach	Beach roll-back and erosion are natural cyclic processes rather than failure Beaches fail when they do not perform their primary function (e.g. overtopping/ tidal flooding/erosion protection), although they may recover with time. Key processes resulting in failure: • Overtopping due to erosion/gullying/reduced energy dissipation following beach lowering • Failure of control structures

Within the scope of the project it was not possible to analyse all indicative failure modes. The failure modes that were selected for analysis for each defence type are listed in table 2.

Table 2 Selected Indicative Failure Modes chosen for analysis

Flood and coastal defence type		Indicative failure/s Mode/s
Embankment / sloping seawall		• Erosion of crest and inside face leading to breach following overtopping. • Piping, excessive seepage (river embankments)
Vertical wall structures	Anchored sheet pile	• Toe erosion dealing to rotation about the tie rod. • Rupture of the tie rod following toe erosion and corrosion.
	Cantilever wall	• Scour on the toe of the sheet pile followed by instability and collapse of the wall.
	Masonry wall	• Overturning of the structure. • Sliding of the structure.
Sand / Shingle Beach		• Breaching of the beach after crest retreat.

1.1 Outline of report

The Performance and Reliability Project (FD2318) ran in parallel to the development of RASP HLM+ for NaFRA 2004. Section 2 explains the methodology followed to create the fragility curves that were used for NaFRA 2004.

Fragility curves for a national level or broad scale flood risk assessment are based on limited data. The need for simplification of a national level risk assessment can never entirely be eliminated; Dekker (1996) and Dekker and Scarf (1998) indicate that the quality of higher level assessments is a common problem in maintenance optimisation systems.

Section 3 describes the models underpinning the fragility curves provided in the annexes of TR1. This methodology builds on the approach used for the NaFRA fragility curves and captures the indicative failure modes from table 2 in more detail. These fragility curves are subject to the same data limitations which requires assumptions and simplifications of the failure mode representations. The approach described in section 3 demonstrates the process to generate a fragility curve, and provides a basis for future improvements of the fragility curves when more data becomes available.

2. Fragility curves for HLM+ Flood risk assessment

The following subsections explain how fragility curves where developed in the Performance and Reliability project for use in NaFRA 2004 and subsequent improvements to these.

2.1 Coastal defences

Keeping the above in mind, the following approach was taken to establish fragility curves for coastal defences for use in national flood risk assessments:

a) System interactions were not in the scope of the fragility curve refinements and remain therefore based on the approach according to Hall *et al*. (2003)
b) A literature review was carried out of the failure modes associated with each of the coastal defence types, see HR Wallingford (2004)
c) A review was carried out in co-operation with practitioners to establish the most prominent failure modes of the different flood and coastal defence types according to their experience (HR Wallingford, 2004). For coastal earth embankments failure due to wave overtopping followed by erosion of the embankment leading to breach was identified as the most prominent failure mode.
d) The limit state function for this failure mode for earth embankment was taken and the coefficients were adapted to capture all types of structures.

The limit state equation for overtopping/overflowing (i.e. when the sea level is above the defence crest level) of coastal defences is based on discharge and defined as:

$$Z = q_c - q_a$$

where:
Z = limit state function such that $Z \leq 0$ represents system failure.
q_c = critical overtopping discharge
q_a = calculated discharge

For the development of the fragility curves, q_a is considered deterministic. The task here is therefore to define q_c. Vrouwenvelder (2001) provides a method for deriving a model to determine q_c. The derivation of this model is detailed in Appendix B of the Literature Review report, with the resulting model defined by the equation below.

$$q_c = \left[\frac{3.8 \cdot c_g^{2/3}}{(6 \cdot 10^5)^{2/3} \cdot \left[1 + 0.8 \cdot \log_{10}\left(P_t \cdot t_s \cdot \frac{c_g \cdot d_w}{c_g \cdot d_w + 0.4 \cdot c_{RK} \cdot L_{K,inside}} \right) \right]} \right]^{5/2} \cdot \frac{k^{1/4}}{125 \cdot (\tan \alpha_i)^{3/4}}$$

where:

- c_g (m·s)= coefficient that represents the erosion endurance of the grass. The values of cg can range from 10^6 ms in case of good quality to $3.3 \cdot 10^5$ ms in case of bad quality.
- P_t = percentage of the time that overtopping/flowing over occurs. In case of flowing over Pt is 1 and in case of overtopping P_t takes the pulsatory character of overtopping in account
- t_s (hours)= duration of the storm
- d_w (m) = the depth of the grass roots. Values of d_w range between 0.05m and 0.07m, factors influencing the magnitude of this factor are: maintenance, location (sea or river embankments) and the type of vegetation.
- c_{RK} (m·s) = coefficient with regard to the erosion endurance of the clay cover layer. The values for c_{RK} range from $7 \cdot 10^3$ m·s (bad quality clay) to $54 \cdot 10^3$ m·s (good quality clay). In case of sand $c_{RK} = 0$.
- $L_{k,inside}$ (m) = width of the inside clay cover layer, that can be considered as the total width of the embankment.
- k (s^6/m^2) = roughness factor according+
- to Strickler of the inside slope.
- α_i (degrees) = angle of the inside slope.

e) The information available for coastal defences was established, in this case the information comes from the National Flood and Coastal Defence Database in the UK:
   - Type of structure
   - Whether the structure is narrow or wide (not quantified)
   - Condition grade 1 to 5, indicating excellent to very poor.

f) The parameters in the critical discharge model were defined. The parameters of the q_c model that are unknown at a national level has to be set up using probabilistic distributions taken from literature or via expert judgement. To define the probabilistic distributions, mean values and standard deviations or variation coefficients (= stdv / mean value) have been taken from Vrouwenvelder *et al*. (2001). An example is given in tables 3 y 4. Considering the degree of knowledge about the parameters actually larger variations should be chosen. However, it was chosen to reflect this uncertainty in the form of upper and lower bands in the fragility curve.

g) Visual inspections expressed in a condition grade are more likely to focus on the state of the vegetation than on the quality of the soil in the embankment. The grass strength in the q_c model was taken as representative for the strength of the structure on the crest and inside slope of the structure. The condition grades are therefore linked to different values of the erosion strength of grass (this value varies if the cover is not grass). A sensitivity analysis was undertaken that proved that this parameter has the most influence on the model. If the structure cover was other than grass then the erosion endurance was multiplied with an extra factor to take that effect into account. Finally, the range of coefficients associated with different degrees of erosion strength were split up to reflect the five condition grades. A different geometry on the outside slope affects the wave run-up and therefore the actual occurring wave overtopping on the loading side of the limit state function rather than the critical discharge values. In the approach based on the limit state function above, different outside geometry makes no

difference in the fragility curve. This difference can be represented varying c_g to represent the erosion endurance of different materials.

Table 3 Distribution functions for the parameters in the q_c model in the national level flood risk assessment

		Distribution function	Standard deviation (σ) or variation coefficient (ν)	Mean
Width L_K	**Narrow (m)**	lognormal	σ = 0.2	7.5
	Wide (m)			20.0
Tan α_i (angle inside slope)	**Steep (tan)**	normal	ν = 0.05	0.5
	Shallow (tan)			0.25
Erosion strength c_g		lognormal	ν = 0.30	See table below
Grass root depth d_w		lognormal	ν = 0.20	0.1
Roughness inside slope k		lognormal	ν = 0.25	0.015
Erosion strength core embankment c_{RK}		lognormal	ν = 0.30	23,000

Table 4 Mean values for the parameters in the q_c model in the national level flood risk assessment for different defence types

Erosion strength c_g: Front face surface protection					
Condition Grade	Embankment		Vertical wall		
	Grass (permeable)	Grass (impermeable)	Gabions	Masonry	Sheet piles
Condition 1	1000000	1500000	1500000	3000000	2500000
Condition 2	850000	1275000	1275000	2550000	2125000
Condition 3	600000	900000	900000	1800000	1500000
Condition 4	415000	622500	622500	1245000	1037500
Condition 5	330000	495000	495000	990000	825000
Erosion strength c_g: Front face and crest surface protection					
Condition Grade	Embankment		Vertical wall		
	Grass (permeable)	Grass (impermeable)	Gabions	Masonry	Sheet piles
Condition 1	1500000	2250000	2250000	4500000	3750000
Condition 2	1275000	1912500	1912500	3825000	3187500
Condition 3	900000	1350000	1350000	2700000	2250000
Condition 4	622500	933750	933750	1867500	1556250
Condition 5	495000	742500	742500	1485000	1237500
Erosion strength c_g: Front face, crest and rear protection					
Condition Grade	Embankment		Vertical wall		
	Grass (permeable)	Grass (impermeable)	Gabions	Masonry	Sheet piles
Condition 1	2000000	3000000	3000000	6000000	5000000
Condition 2	1700000	2550000	2550000	5100000	4250000
Condition 3	1200000	1800000	1800000	3600000	3000000
Condition 4	830000	1245000	1245000	2490000	2075000
Condition 5	660000	990000	990000	1980000	1650000

h) Calculating the fragility curve. For RASP HLM+, due to time constrains, the fragility curves were calculated defining a variation coefficient and distribution function of the results of the limit state function. These probabilistic parameters were estimated taking into account the influence on the results of the variation coefficient and distribution of all the parameters of the model. Later on in the project, the fragility curves were improved using probabilistic programmes that undertake Monte Carlo simulations, making sure that sufficient simulations are performed.

2.2 Fluvial defences

In fluvial areas waves are not normally a dominant aspect in the loading of flood defence structures. The main loading parameter in the fragility curve is therefore the loading-level and not the wave overtopping discharge. The loading-level is defined as the difference between the water level and the crest level of the defence. If the loading-level is positive, the river water level exceeds the crest level, resulting in an overflow discharge causing erosion to the rear

slope. The probability of failure due to overflow can be derived based on the same critical discharge model and parameters as applied for coastal defences.

The critical water level minus crest level value for which breach of the embankment occurs Δh_c can be determined as follows (broad crested weir equation):

$$\Delta h_c = \sqrt[3]{\frac{2.78 \cdot q_c^2}{g}}$$

Negative and low positive water level minus crest level values do not result in failure of the defence due to erosion. However, negative and low positive water level minus crest level values are connected to relatively high water levels and can result in failure due to for instance piping or instability of the inside slope. Failure due to piping is taken as indicative for this range of water level minus crest level values. The following limit state function based on Terzaghi's model (Terzaghi and Peck, 1967) is taken:

$Z = dh_c - dh$

In which

- dh_c = critical head difference between the river water level and the water level in the hinterland resulting in piping if exceeded.
- dh = actual occurring head difference between the river water level and the water level in the hinterland.

The critical head difference is expressed as follows:

$$dh_c = \frac{t + \frac{1}{3}L}{C_w}$$

In which (Figure 2)

- t is the thickness of the impervious layers underneath the embankment,
- L is the horizontal seepage length reaching from the point in the river where the water conductive sand layer is in contact with the river water level to a weak point behind the embankment formed by e.g. a ditch where uplifting of the impervious layer might occur,
- C_w is the creep ratio, which takes on different values in relation to the soil type.

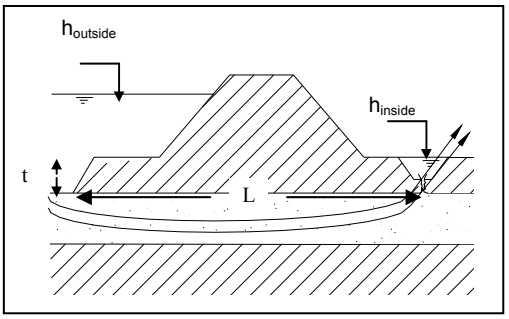

Figure 2 Piping underneath embankment

To simplify matters, the inside and outside toe of the embankment are assumed to be on the same level. The inside water level is assumed to be at the level of the inside toe. The outside water level is then equal to the water head difference. The loading-level values associated with the head difference ‘dh’ can be derived by subtracting the crest level from ‘dh’.

This approach by taking piping underneath the embankment is not wholly representative of the type of piping failure that is expected to occur in the UK - piping through the embankment is more often found.

The probability of failure due to piping through the embankment is a combination of:

- the probability of failure due to piping through the embankment itself
- the probability that fluvial embankments are deteriorated due to animal infestation or weakened by the presence of a permeable stratum in the embankment, or fissured or cracked material
- preferential seepage routes at interfaces between the embankment and point structures

Reliable models that represent these processes do not yet exist and so for fragility calculation the approach adopted was for the probability of failure due to piping (through the embankment) was calculated assuming that the thickness of the impervious layers underneath the embankment (parameter t) is zero and the distance L is equal to the width of the embankment.

The probability of finding a weak stratum or a stratum deteriorated by infestation will be taken into account multiplying the probability of failure by the probability of this situation occurring.

Table 5 Parameters and distribution functions for fluvial embankments

		Distribution function	Standard deviation (σ) or variation coefficient (ν)	Mean
Width L_K	**Narrow (m)**	lognormal	σ = 0.2	7.5
	Wide (m)			20.0
Tan α_i (angle inside slope)	**Steep (tan)**	normal	ν = 0.05	0.5
	Shallow (tan)			0.25
Erosion strength c_g		lognormal	ν = 0.30	See table below
Grass root depth d_w		lognormal	ν = 0.20	0.1
Roughness inside slope k		lognormal	ν = 0.25	0.015
Erosion strength core embankment c_{RK}		lognormal	ν = 0.30	23,000
t, thickness impervious layers		normal	σ = 2.5	0
C_w creep ratio		normal	σ = 0.2	
Seepage length L (m)	Condition 1	normal	σ = 0.2	60
	Condition 2			60
	Condition 3			60
	Condition 4			10
	Condition 5			6

Fragility curve

The fragility curve for fluvial defences is based on the limit state functions and the corresponding parameter values as explained above. The critical discharge in the overtopping limit state function and the critical head difference in the piping limit state function is transformed into critical water level minus crest level values.

The probabilities of failure given the water level minus crest level are calculated with both limit state functions using Montecarlo (as explained above, for RASP HLM+ the fragility curves were calculated defining a variation coefficient and distribution function of the results of the limit state function). The probability of failure of the flood defence is the addition of the probability of failure due to both modes and considering them independent.

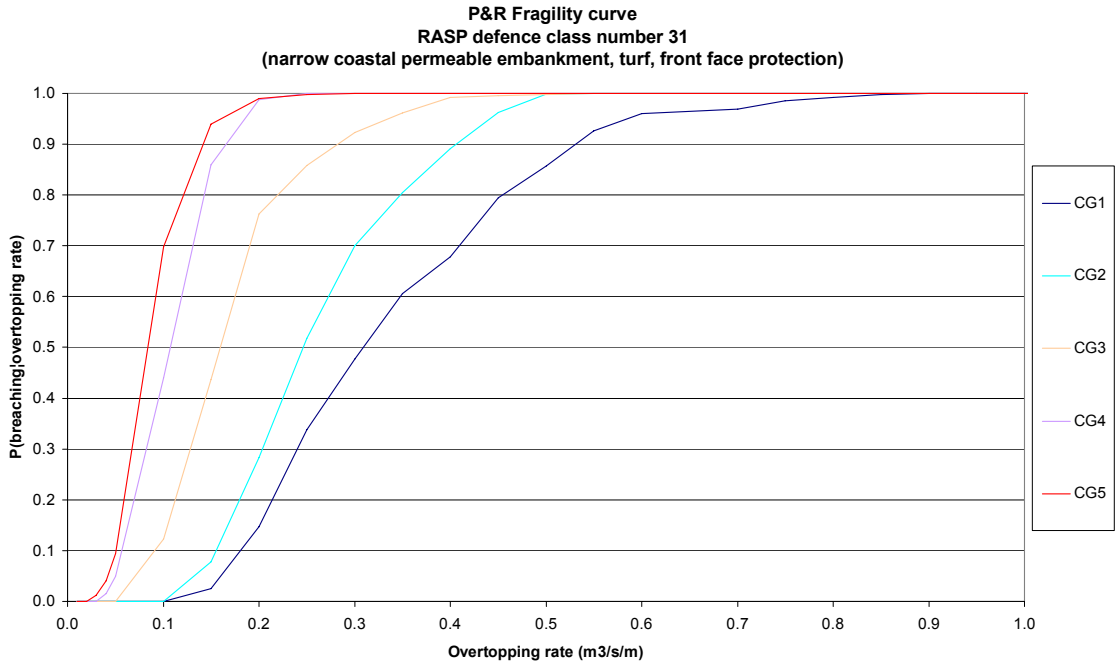

Figure 3 Example of fragility curve for coastal defence

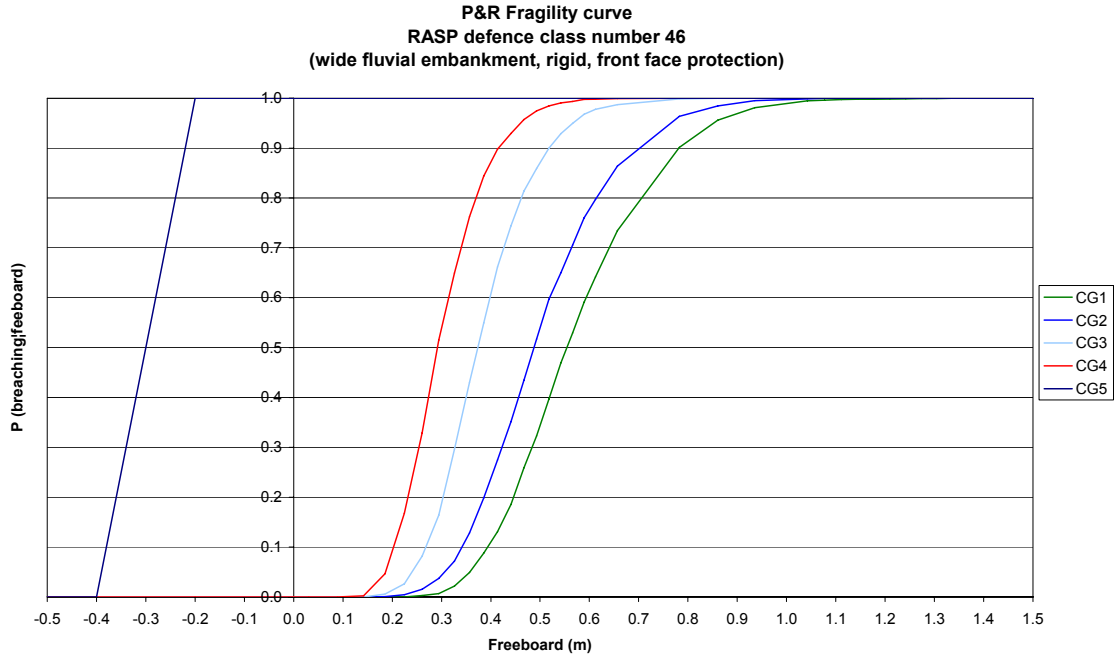

Figure 4 Example of fragility curve for fluvial defence

3. Introduction to more detailed representations of indicative failure modes in fragility curves

This section describes the models underpinning the fragility curves provided in the annexes of TR1. This methodology builds on the approach used for the NaFRA fragility curves and captures the indicative failure modes from table 2 in more detail. These fragility curves are subject to the same data limitations which requires assumptions and simplifications of the failure mode representations. The approach described in this section demonstrates the process to generate a fragility curve and provides a basis for improvements of the fragility curves when more data become available.

The following considerations are important to this section:

- The limit state functions have been developed for an indicative failure mode. This indicative failure mode was identified in prior stages of the project as the most common one, see table 2.
- In some cases two failure modes have been studied as both of them have an important influence in the failure of the type of defence under study. The total probability of failure of the flood defence in this case will be the addition of the probability of failure due to both failure modes and considering them independently.
- For each defence type the information known at the highest level of decision making is listed. For more detailed assessments more detailed information will be known.

The approach developed in this section is fine-tuned to situations with low data availability. The models, and e.g. failure mode dependencies, should therefore be revisited when moving towards more detailed assessments.

3.1 Embankments

Figure 5 illustrates a selection of typical failure mechanisms for embankments.

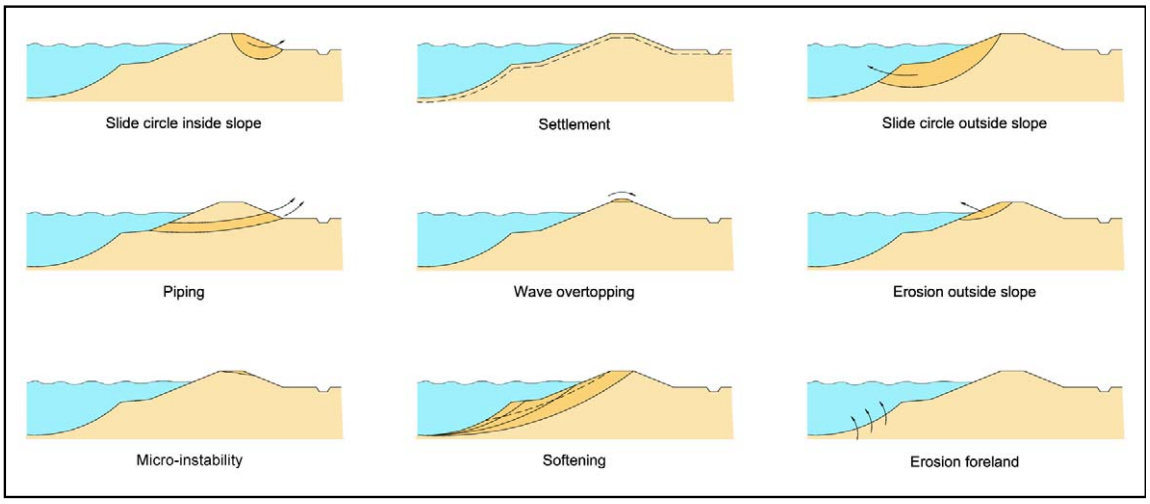

Figure 5 Typical failure mechanisms for embankments. (from TAW, 1999).

The key failure modes of embankments identified from the consultation process with practitioners are shown in Table 1.

From the list of key failure modes, failure via overtopping was identified as being the indicative failure mode for embankments. The methodology to build fragility curves for this failure mode is the same explained in TR1, Section 3, for high level risk assessment. The difference will be in the input data used, as at intermediate and low levels of risk assessment more information will be available and the uncertainty of the parameters will be lower.

3.1.1 Coastal embankments

The approach taken to establish fragility curves for coastal earth embankments is similar to the one used for high level of risk assessment explained in TR1, Section 3. The differences are in the input data.

The model to use is repeated below (Vrouwenvelder, 2001):

$$q_c = \left[\frac{3.8 \cdot c_g^{2/3}}{(6 \cdot 10^5)^{2/3} \cdot \left[1 + 0.8 \cdot \log_{10}(P_t \cdot t_s \cdot \frac{c_g \cdot d_w}{c_g \cdot d_w + 0.4 \cdot c_{RK} \cdot L_{K,inside}}) \right]} \right]^{5/2} \cdot \frac{k^{1/4}}{125 \cdot (\tan \alpha_i)^{3/4}}$$

Where

- c_g (m·s)= coefficient that represents the erosion endurance of the grass. The values of c_g can range from 10^6 ms in case of good quality to $3.3 \cdot 10^5$ ms in case of bad quality.
- P_t = percentage of the time that overtopping/flowing over occurs. In case of flowing over P_t is 1 and in case of overtopping P_t takes the pulsatory character of overtopping in account
- t_s (hours)= duration of the storm
- d_w (m) = the depth of the grass roots. Values of d_w range between 0.05m and 0.07m, factors influencing the magnitude of this factor are: maintenance, location (sea or river embankments) and the type of vegetation.
- c_{RK} (m·s) = coefficient with regard to the erosion endurance of the clay cover layer. The values for c_{RK} range from $7 \cdot 10^3$ m·s (bad quality clay) to $54 \cdot 10^3$ m·s (good quality clay). In case of sand $c_{RK} = 0$.
- $L_{k,inside}$ (m) = width of the inside clay cover layer, that can be considered as the total width of the embankment.
- k (s^6/m^2) = roughness factor according to Strickler of the inside slope.
- α_i (degrees) = angle of the inside slope.

An example of a fragility curve has been built using the same mean values and probabilistic distribution functions as those used in Figure 3 but with lower values of standard deviation to capture the uncertainty reduction in the parameter's values (narrow coastal permeable embankment front face protection). The values used to build the fragility curves are shown in Table 6 and the fragility curves are shown in Figure 6.

Table 6 Example of parameters and distribution functions for coastal embankment fragility curves for intermediate levels of risk assessment

		Distribution function	**Standard deviation (σ) or variation coefficient (ν)**	**Mean**
Width L_K	**Narrow (m)**	lognormal	σ = 0.1	7.5
	Wide (m)			20.0
Tan α_i (angle inside slope)	**Steep (tan)**	normal	ν = 0.025	0.5
	Shallow (tan)			0.25
Erosion strength c_g		lognormal	ν = 0.15	See table below
Grass root depth d_w		lognormal	ν = 0.10	0.1
Roughness inside slope k		lognormal	ν = 0.125	0.015
Erosion strength core embankment c_{RK}		lognormal	ν = 0.15	23,000

Erosion strength c_g: Front face surface protection					
Condition Grade	Embankment		Vertical wall		
	Grass (permeable)	Grass (impermeable)	Gabions	Masonry	Sheet piles
Condition 1	1000000	1500000	1500000	3000000	2500000
Condition 2	850000	1275000	1275000	2550000	2125000
Condition 3	600000	900000	900000	1800000	1500000
Condition 4	415000	622500	622500	1245000	1037500
Condition 5	330000	495000	495000	990000	825000

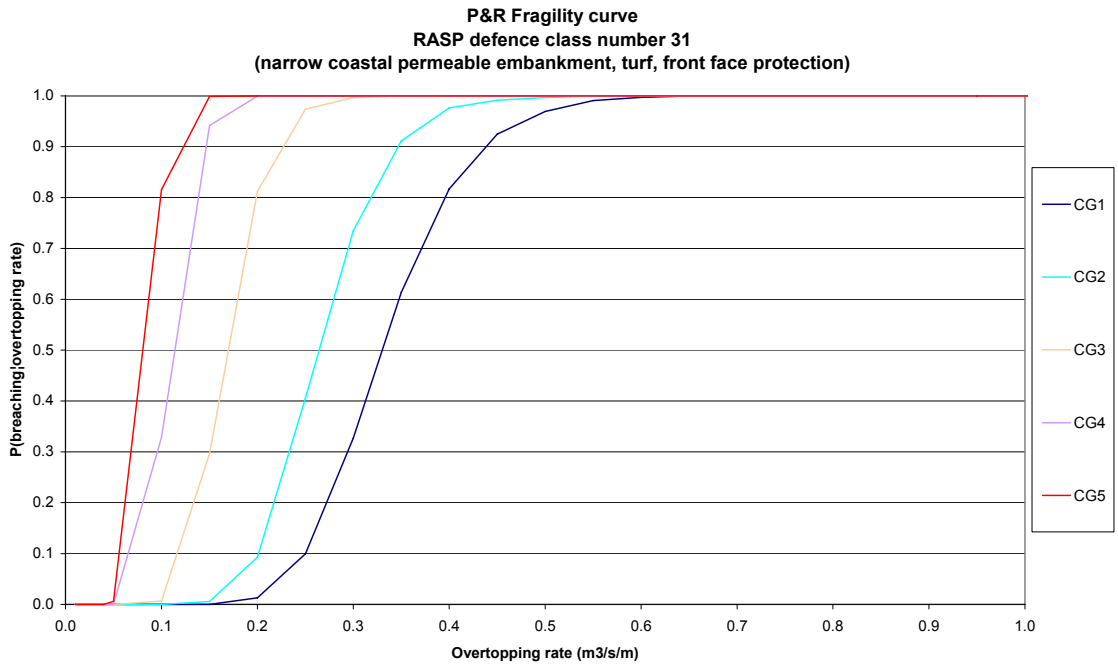

Figure 6 Example coastal embankment fragility curve for intermediate levels of risk assessment

When comparing Figures 3 and 6 you will observe that the fragility curves are more vertical when uncertainty is lower. In the ideal case in which all the parameters are perfectly known, the fragility curve would be a vertical line for a given overtopping rate.

3.1.2 Fluvial embankments

Limit state function

As for coastal embankments, the fluvial embankment fragility curves have similarly been developed using the same model as that used for the national flood risk assessment.

An example of a fragility curve has been built using the same mean values and probabilistic distribution function as those used in Figure 4 but with lower values of standard deviation.

Table 7 Example of parameters and distribution functions for fluvial embankment fragility curves and intermediate levels of risk assessment.

		Distribution function	Standard deviation (σ) or variation coefficient (ν)	Mean
Width L_K	**Narrow (m)**	lognormal	σ = 0.1	7.5
	Wide (m)			20.0
Tan α_i (angle inside slope)	**Steep (tan)**	normal	ν = 0.025	0.5
	Shallow (tan)			0.25
Erosion strength c_g		lognormal	ν = 0.15	See table below
Grass root depth d_w		lognormal	ν = 0.10	0.1
Roughness inside slope k		lognormal	ν = 0.125	0.015
Erosion strength core embankment c_{RK}		lognormal	ν = 0.15	23,000
t, thickness impervious layers		normal	σ = 1.25	0
C_w creep ratio		normal	σ = 0.1	
Seepage length L (m)	Condition 1	normal	σ = 0.1	60
	Condition 2			60
	Condition 3			60
	Condition 4			10
	Condition 5			6

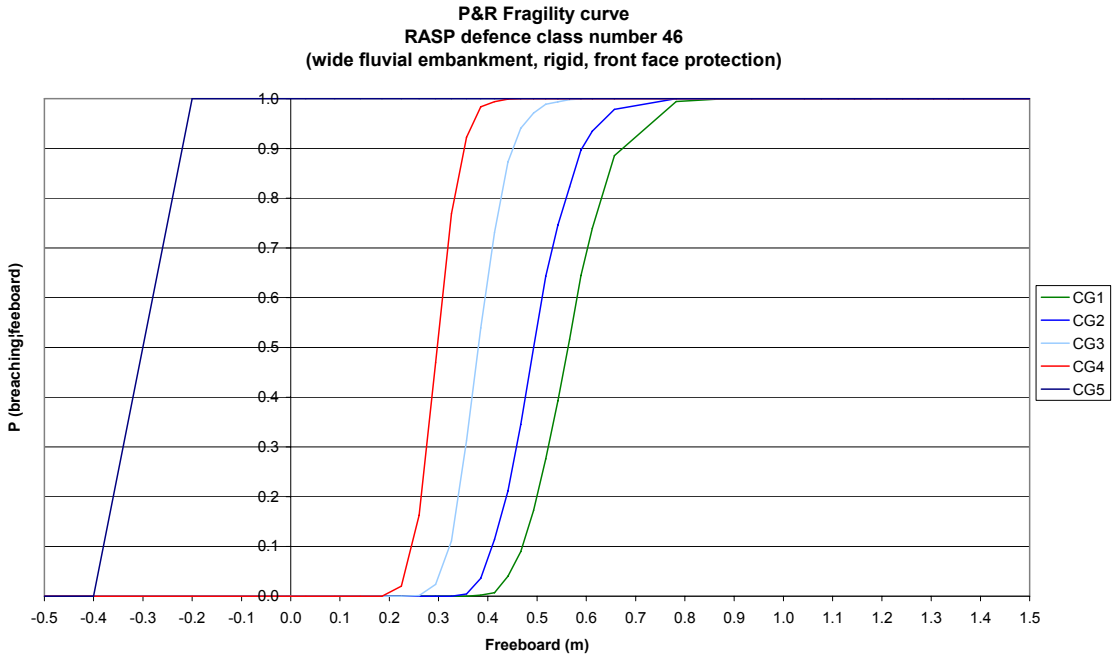

Figure 7 Example fluvial embankment fragility curve for intermediate level of risk assessment

3.2 Fragility anchored sheet piles

3.2.1 Limit state functions

Two failure modes are taken as indicative of the probability of failure of anchored sheet pile walls:

a) Rotation about the tie rod
b) Rupture of the tie rod

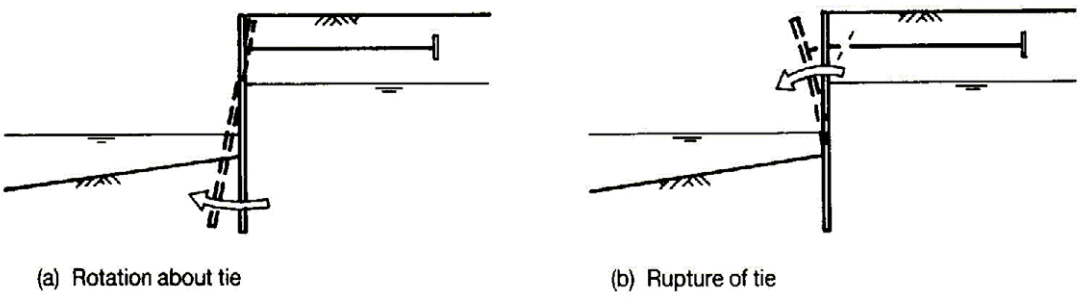

Figure 8 Indicative failure modes of anchored sheet piles

The following steps are taken to determine the probability of failure of the structure:

1. Rotation about the tie rod

The main forces on the sheet pile wall are given in the figure below.

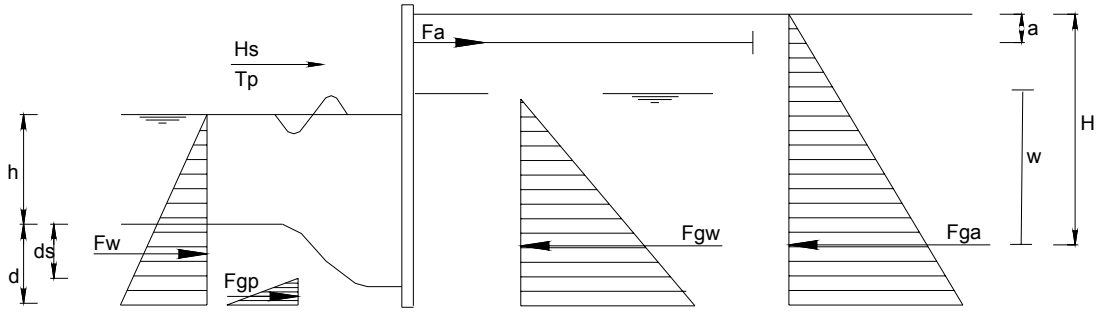

Figure 9 Main forces acting on anchored sheet piles

- Horizontal hydraulic force of the water that saturates the ground

$$F_{gw} = \frac{1}{2} \cdot \gamma_w \cdot (w+d)^2$$

if h>H then w = h

$$F_{gw} = \frac{1}{2} \cdot \gamma_w \cdot (h+d)^2$$

- Horizontal force exerted by the ground behind the structure.

$$F_{ga} = K_a \cdot \frac{1}{2} \cdot \gamma_b \cdot (H-w)^2 + K_a \cdot \gamma_b \cdot (H-w) \cdot (w+d) + \frac{1}{2} \cdot \gamma_s \cdot K_a \cdot (w+d)^2$$

if h>H then w = H

$$F_{ga} = \frac{1}{2} \cdot \gamma_s \cdot K_a \cdot (H+d)^2$$

- Horizontal passive force exerted by the ground in front of the structure.

$$F_{gp} = K_p \cdot \frac{1}{2} \cdot (\gamma_s) \cdot (d-d_s)^2$$

if $d_s > d$, $F_{gp} = 0$

- Horizontal hydraulic force, which has a stabilising effect on the structure.

$$F_w = \frac{1}{2} \gamma_w (h+d)^2$$

if h>H then w = h

$$F_{gw} = \frac{1}{2} \cdot \gamma_w \cdot (h+d)^2$$

where

H = retaining height before scour occurring (m)
a = depth of the anchor below the ground level (m)
x = locates the maximum moment on the sheet pile wall (m)
d = depth of the toe of the sheet pile wall (m)
d_s = depth of the scour hole as function of the wave action (m) = 20% water level (m)
F_{ga} = resulting active horizontal ground force (kN)
F_{gw} = resulting horizontal force due to the water in the ground (kN)
F_{gp} = resulting passive horizontal ground force due to the ground that has not scoured (kN)
F_w = resulting horizontal force exerted by the water (kN)
F_a = force exerted by the anchor (kN)
w = water level in the ground above the channel bed
γ_b = bulk density of the ground (kN/m^3)
γ_s = submerged density of the ground (kN/m^3)
γ_w = water density (kN/m^3)
w = water level in the ground above the channel bed (m)

The limit state function is:

$L_{rot} = \Sigma M(+) - \Sigma M(-) > 0$
Where
M(+) = anticlockwise moments about the tie rod when scour has taken place.
$\Sigma M(+) = MF_w + MF_{gp}$

M(-) = clockwise moments about the tie rod when scour has taken place.
$\Sigma M(-) = MF_{ga} + MF_{gw}$

2. Rupture of the tie

- Determine the force in the anchor, $F_a(d_s=0)$, given the design hydraulic loading conditions and appropriate safety coefficient. This is done by determining the horizontal forces on the sheet pile. The resulting horizontal force must be zero.

  $$F_a + F_w + F_{gp} - F_{ga} - F_{gw} = 0$$

- If the tie rod section is unknown, it can be determined using the design force in the anchor calculated above.

  $$F_a = S \cdot f/SC$$

  where:
  S = design section of the tie rod (m^2)
  f = yield stress of the tie rod (kg/m^2)
  SC = safety coefficient used during design (usually taken as 2)

- Determine the real tie rod section after corrosion has taken place.

$$S = \pi \cdot r^2$$
$$r_c = r - (c \cdot y)$$
$$S_c = \pi \cdot r_c^{\,2} = \pi \cdot \left(\sqrt{\frac{S}{\pi}} - (c \cdot y) \right)^2$$

Where
S = section before corrosion has taken place
r = radio before corrosion has taken place
S_c = section after corrosion has taken place
r_c = radio after corrosion has taken place
c = corrosion rate per year
y = number of years

- Determine the real force in the anchor after scour has taken place $F_a(d_s)$

  $F_a(d_s) = F_{gw} + F_{ga} - (F_w + F_{gp})$

- Determine the force that the anchor can bear after corrosion has taken place F_c

  $F_c = S_c \cdot f$

The probability of failure by rupture of the tie is:
$P(L) < 0$
$L_{rup} = F_c - F_a(d_s)$

The probability of failure of the flood defence will be the addition of the probability of failure due to both modes and considering them independent.

Depth of the scour

Coastal structures: The depth of the scour hole, d_s, given the hydraulic loading conditions can be determined based on:

Table 8 Methods to determine the depth of scour

Toe scour depth, two options (McConnell 1998)	
Depth of scour, d_s $d_s = H_{max}$ where: H_{max} - maximum unbroken wave height (m) $= 1.8 H_s$ H_s - significant wave height (m)	Depth of scour, d_s d_s - from prediction graphs for scour depth, after Powell (1989)

River flood defences:
There is not a developed method to determine the scour produced on flood defences along river channel. A “rule of thumb” of the maximum scour produced

during a flood event is to consider the depth of the scour equal to 20% the flood depth.

3.2.2 Condition grades

For the condition grades

One of the main deterioration processes of (anchored) sheet pile walls is ALWC in the splash zone. However, this does not relate directly to the rotation based failure mode developed above. Therefore, the moment on the strength side in the limit state function of the sheet pile wall is reduced using a factor resp. 1.0, 0.8, 0.6, 0.4, 0.2

3.2.3 Data requirements

Some deliberations with respect to the data requirements are described below :

- Water level h(m): the water level is at the same time a destabilising force (given that the scour is proportional to the water level) and a stabilising force. In terms of the limit state equation, this means that the strength of the structure is also dependent on the loading parameter so it is not possible to separate strength from load as in the fragility curves developed for embankments.
  a. For a fluvial environment the scour (load) is also dependent on the velocities of the flow (function of the water level) on the channel. On the view of this dependencies there are two situations in which the probability of failure is higher:
     - when the water level is very high: the scour is bigger, which is a destabilising factor.
     - when the water level is very low: the establishing force exerted by the water pressure F_w (M_{Fw}) is also low, which is a stabilising factor.
  b. For coastal structure, higher water levels have a stabilising effect. High waves result in deeper scour holes. The most unfavourable combination of events is therefore a storm with high wind speeds during low water of the tide. The high wind speeds inevitably lead to a surge. Return periods of high water levels are associated with high water tide events and surge. Large high water events of tides are associated with tides with large amplitudes and are therefore also associated with relatively small low water events. The return period of the high water levels therefore also apply to relatively small low water events combined with a relatively high surge (in other words high wind speeds). The high water levels can be transformed into low water levels by subtracting twice the amplitude of the tidal event. Low water plus surge is what remains and what should be considered as most unfavourable situation.
     - Wall exposed height H(m): This value is known (deterministic) based on local knowledge or from NFCDD.
     - Depth of the anchor a(m): This value is difficult to estimate if not known. Design manuals usually recommend to place the anchor minimum 1 m below the ground level behind the structure. Uncertainty on this value should be captured associating a probabilistic distribution function to it or defining uncertainty bands.

- Ground density: average values depending on the ground type can be defined from literature. When this density is unknown, Vrouwenvelder *et al*. (2001) recommends to use the following:

Table 11 Ground density probabilistic parameters

	Distribution function	Mean value	Variation coefficient
Ground submerged density γ_s (kN/m^3)	normal	Depending on ground type (kN/m3)	V = 0.05
Ground bulk density γ_g (kN/m^3)	normal	Depending on ground type (kN/m3)	V = 0.05

- Water density: typical values are 10 kN/m^3 for drinking water and 10.3 kN/m^3 for sea water.
- Yield stress of the tie rod: Mean values for different steel types can be taken from BS 4360. CUR 190 recommends to use the following probabilistic parameters a variation coefficient

Table 12 Steel yield stress probabilistic parameters

	Distribution function	Mean value	Variation coefficient
Yield stress of the tie rod (kg/m^2)	lognormal	f_y (kg/m^2) = BS 4360 (High Yield Steel) Grade 50B & 50C	V =0.10 (CUR 190)

- Cut-off depth: The cut-off length of the sheet pile wall is usually unknown. The method that is recommended to apply to estimate it is the “free earth support” method. The condition is that the penetration of the piles is such that the passive pressure in front of the piles is sufficient to resist the forward movement of the toes of the piles, but not sufficient to prevent rotation (which is prevented by the ties at the top of the walls). Scour at the toe of the sheet pile wall causes the soil passive pressure at the toe of the sheet pile wall to decrease (increasing the probability of rotation around the tie happening) and the stress on the tie to be increasingly loaded (increasing the probability of rupture of the tie rod). Based on local knowledge of the structure and design methods, other methods could be applied to estimate the cut-off length.

3.3 Cantilever walls (non anchored walls)

3.3.1 Limit state function

Cantilever walls are dependent solely upon de penetration of the sheet piling into the soil. The failure mode that is considered to be indicative of the probability of failure of cantilever walls is scour at the toe of the sheet pile wall followed by instability and collapse of the wall by turning around its lowest point. The way in which instability occurs is different from that of an anchored sheet pile wall as the tie rod is not introducing an extra stabilising force.

The limit state function is therefore expressed as follows:

$$L = M_R - M_g$$

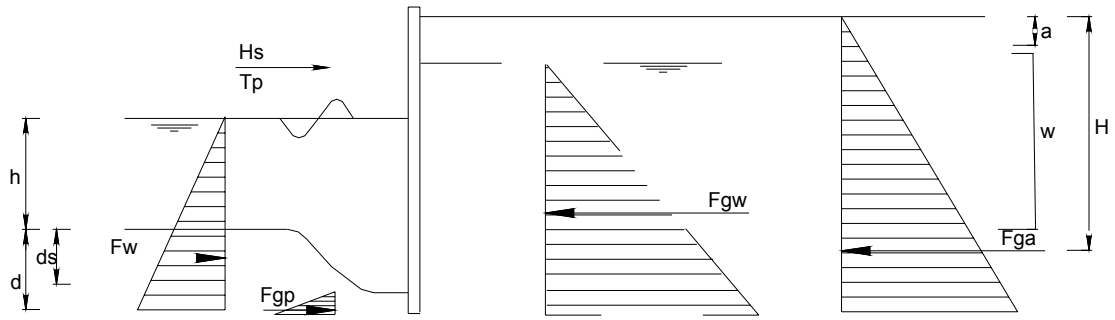

Figure 10 Main forces acting on cantilever walls

In which
M_R = stabilising moment around the lowest point of the cantilever wall introduced by the water level and the passive ground force exerted by the remaining ground body which is not scoured
M_g = destabilising moment introduced by the retained ground and the groundwater.

The forces and moments that act in the system are defined as follows:

- Horizontal force exerted by the ground behind the structure.

$$F_{ga} = K_a \cdot \frac{1}{2} \cdot \gamma_b \cdot (H-w)^2 + K_a \cdot \gamma_b \cdot (H-w) \cdot (w+d) + \frac{1}{2} \cdot \gamma_s \cdot K_a \cdot (w+d)^2$$

$$M_{F_{gs}} = K_a \cdot \frac{1}{2} \cdot \gamma_b \cdot (H-w)^2 \cdot \left(\frac{1}{3} \cdot (H-w) + (w+d) \right) + K_a \cdot \gamma_b \cdot (H-w) \cdot (w+d) \cdot \left(\frac{1}{2} \cdot (H+d-w) \right)$$

$$+ \frac{1}{2} \cdot \gamma_s \cdot K_a \cdot (w+d)^2 \cdot \left(\frac{1}{3} \cdot (w+d) \right)$$

if h > H then w = H

$$F_{ga} = \frac{1}{2} \cdot \gamma_s \cdot K_a \cdot (H+d)^2$$

$$M_{F_{gs}} = \frac{1}{2} \cdot \gamma_s \cdot K_a \cdot (w+d)^2 \cdot \left(\frac{1}{3} \cdot (H+d) \right)$$

- Horizontal hydraulic force of the water that saturates the ground

$$F_{gw} = \frac{1}{2} \cdot \gamma_w \cdot (w+d)^2$$

$$M_{F_{gw}} = \frac{1}{6} \cdot \gamma_w \cdot (w+d)^3$$

if h > H then w = h

$$F_{gw} = \frac{1}{2} \cdot \gamma_w \cdot (h+d)^2$$

$$M_{F_{gw}} = \frac{1}{6} \cdot \gamma_w \cdot (h+d)^3$$

- Horizontal hydraulic force, which has a stabilising effect on the structure. This moment is defined as follows:

$$F_w = \frac{1}{2} \cdot \gamma_w \cdot (h+d)^2$$

$$M_{F_w} = \frac{1}{6} \cdot \gamma_w \cdot (h+d)^3$$

- Horizontal passive force exerted by the ground in front of the structure.

If $d_s < d$

$$F_{gp} = \frac{1}{2} K_p \cdot \gamma_s \cdot (d-d_s)^2$$

$$M_{F_{gp}} = \frac{1}{2} \cdot \gamma_s \cdot (d-d_s)^2 \cdot K_p \cdot \frac{1}{3} \cdot (d-d_s)$$

If $d_s > d$

$$F_{gp} = 0$$

$$M_{F_{gp}} = 0$$

The components of the limit state function are:

$\Sigma M_R = M_{Fgp} + M_{Fw}$

$\Sigma M_g = M_{Fga} + M_{Fgw}$

In these equations:

H = height of the earth embankment behind the structure (m)
d_s = depth of the scour hole caused by the waves (m0)
d = depth of the base of the structure with respect to the elevation of the bottom (m)
h = water level (m)
d = depth of the base of the structure with respect to the elevation of the bottom (m)
γ_w = volumetric weight of the water (kN/m3)
γ_g = density of the dry soil (kN/m3)
γ_s = density of the saturated soil (kN/m3)
K_a = coefficient applied to get the horizontal active ground force
K_a = coefficient applied to get the horizontal passive ground force

Again, all parameters values are either available or reasonably representative estimates can be made except for the depth of the cantilever wall which is unavailable in the databases.

Depth of the scour

As defined for anchored sheet piles above.

Condition grades

One of the main deterioration processes of (anchored) sheet pile walls is ALWC in the splash zone. However, this does not relate directly to the rotation based failure mode developed above. Therefore, the moment on the strength side in the limit state function of the sheet pile wall is reduced using a factor resp. 1.0, 0.8, 0.6, 0.4, 0.2

3.3.2 Data requirements

Some deliberations on the data requirements are listed below:

a. Water level h(m): the water level is at the same time a destabilising force (given that the scour is proportional to the water level) and a stabilising force. In terms of the limit state equation, this means that the strength of the structure is also dependent on the loading parameter so it is not possible to separate strength from load as in the fragility curves developed for embankments.
b. For a fluvial environment the scour (load) is also dependent on the velocities of the flow (function of the water level) on the channel. On the view of this dependencies there are two situations in which the probability of failure is higher:
   - when the water level is very high: the scour is bigger, which is a destabilising factor.
   - when the water level is very low: the establishing force exerted by the water pressure F_w (M_{Fw}) is also low, which is a stabilising factor.
c. For coastal structure, higher water levels have a stabilising effect. High waves result in deeper scour holes. The most unfavourable combination of events is therefore a storm with high wind speeds during low water of the tide. The high wind speeds inevitably lead to a surge. Return periods of high water levels are associated with high water tide events and surge. Large high water events of tides are associated with tides with large amplitudes and are therefore also associated with relatively small low water events. The return period of the high water levels therefore also apply to relatively small low water events combined with a relatively high surge (in other words high wind speeds). The high water levels can be transformed into low water levels by subtracting twice the amplitude of the tidal event. Low water plus surge is what remains and what should be considered as most unfavourable situation.
   - Wall exposed height H(m): This value is known (deterministic) based on local knowledge or from NFCDD.
   - Ground density: average values depending on the ground type can be defined from literature. When this density is unknown, Vrouwenvelder *et al*. (2001) recommends to use the following the parameter on table 11.
   - Water density: typical values are 10 kN/m^3 for drinking water and 10.3 kN/m^3 for sea water.

– Cut-off depth of the cantilever wall: The depth of the cantilever wall (d) can be calculated using the general design process for Cantilever walls. The condition is that the penetration of the piles is such that the passive pressure in front of the piles is sufficient to resist the rotation of the wall. In reality rotation of the wall does not take place around the lowest point of the wall, so the value of d is then increased 20% to allow for this simplification.

3.4 Masonry walls / Concrete walls / Gabions walls

3.4.1 Limit state function

Mass walls are suitable for retained heights up to 3 m. They can be designed satisfactory for greater heights, but as the height increases other types of walls become more economic.

The interviews with practitioners undertaken during the first stage of the project pointed out that vertical wall structures are considered to be likely to fail due to toe erosion. The two failure modes that might follow to scour of the toe are:

a) Overturning of the structure after scour has taken place at the toe. Another issue is that toe erosion can also pose a threat to the masonry or concrete wall itself after the structure protecting the toe has failed. This effect is considered related to the condition grade of the structure.
b) Sliding of the structure after scour has taken place at toe.

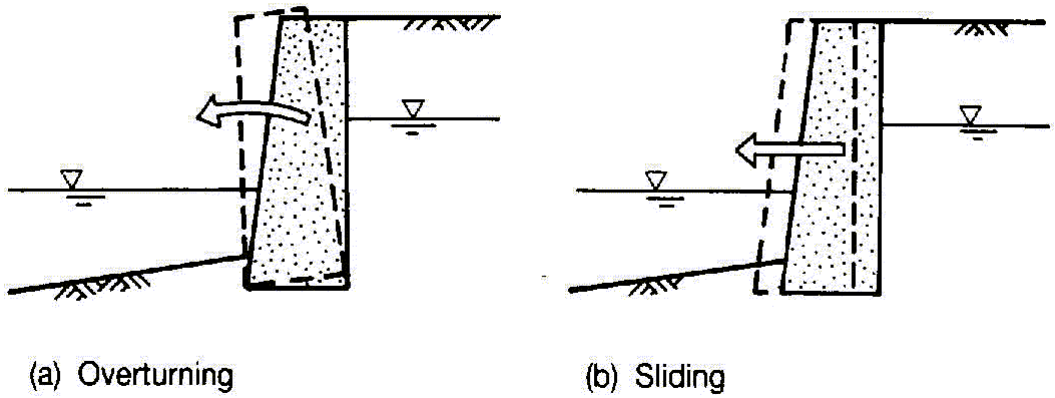

Figure 11 Indicative failure modes of gravity walls

1. Overturning: Tilting of the structure is marked by the occurrence of tensile stress at one of the edges of the base of the structure. Tilting does not occur when the pressures are negative; this is generically expressed as follows:

$$-\frac{\Sigma V}{Bl}+\frac{\Sigma M}{\frac{1}{6}B^2 l}\leq 0$$

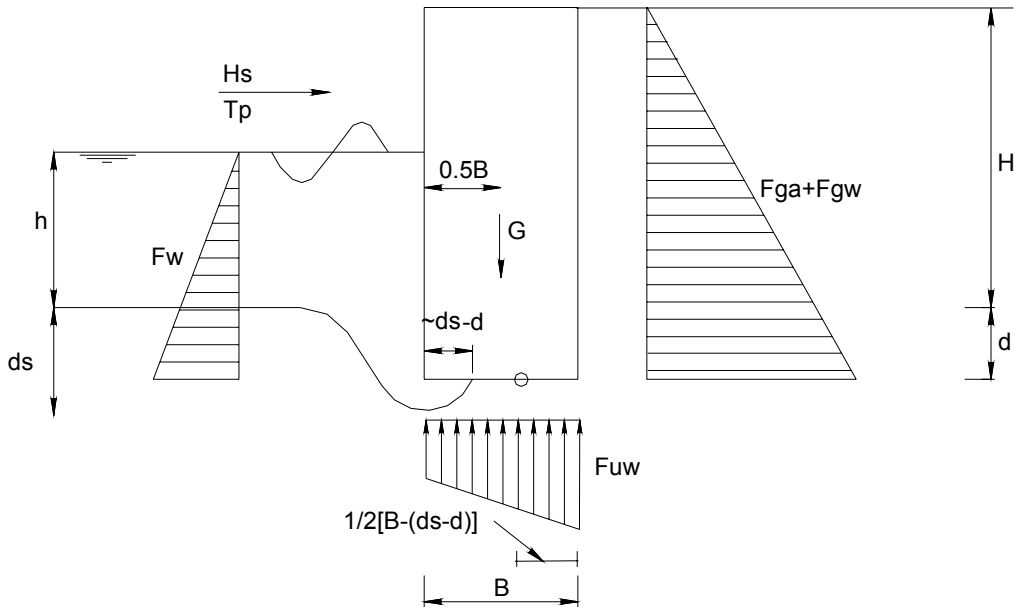

Figure 12 Main forces acting on gravity walls

Where:
ΣV = resulting vertical force, introduced by the weight of the structure and the upward hydraulic pressures (kN)
ΣM = resulting moment on the vertical structure about the centre of the base (kNm)
B = width of the foundation (m)
l = length of the foundation, in this approach taken to equal 1 (i.e. per stretching meter).

Some shifting around of the above equation leads to the following equation:

$$\frac{\Sigma M}{\Sigma V} \leq \frac{1}{6} B$$

This equation is the basis for the limit state function:

$$L = \frac{1}{6} B - \frac{\Sigma M}{\Sigma V}$$

This equation means that to ensure that the base pressure remains compressive over the entire base width, the resultant of the force acting on the base of the wall must act within the middle third of the base, i.e the eccentricity of the base resultant must not exceed B/6. If this rule is observed, adequate safety against overturning of the wall will also be ensured.

In a coastal environment waves during a storm cause a scour hole at the toe of the gravity based structure. In a fluvial situation, the scour is related to the flow velocities of the stream. The scour hole develops underneath the base of the wall and reduces the surface of the base of the wall, which is supported by the underlying foundation of the soil. The loading (the weight of the structure, the

horizontal ground force, the horizontal hydraulic force) of the structure therefore has to be distributed over a decreasing foundation surface. Relating to the limit state function above, the developing scour hole results in a decreasing B.

The forces and moments that act in the system are defined as follows:

- Horizontal force exerted by the ground behind the gravity based structure.

$$F_{ga} = \frac{1}{2} K_a \cdot \gamma_s \cdot (H+d)^2 + K_a \cdot q$$

$$M_{F_{gs}} = \frac{1}{6} \cdot \gamma_s \cdot (H+d)^3 \cdot K_a + K_a \cdot q \cdot \frac{1}{2} \cdot (H+d)$$

- Horizontal hydraulic force of the water that saturates the ground

$$F_{gw} = \frac{1}{2} \cdot \gamma_w \cdot (H+d)^2$$

$$M_{F_{gw}} = \frac{1}{6} \cdot \gamma_w \cdot (H+d)^3$$

if h > H then H = h

$$F_{gw} = \frac{1}{2} \cdot \gamma_w \cdot (h+d)^2$$

$$M_{F_{gw}} = \frac{1}{6} \cdot \gamma_w \cdot (h+d)^3$$

- Horizontal hydraulic force, which has a stabilising effect on the structure. This moment is defined as follows:

$$F_w = \frac{1}{2} \cdot \gamma_w \cdot (h+d)^2$$

$$M_{F_w} = \frac{1}{6} \cdot \gamma_w \cdot (h+d)^3$$

- Horizontal passive force exerted by the ground in front of the structure.

If $d_s < d$

$$F_{gp} = \frac{1}{2} K_p \cdot \gamma_s \cdot (d-d_s)^2$$

$$M_{F_{gp}} = \frac{1}{2} \cdot \gamma_s \cdot (d-d_s)^2 \cdot K_p \cdot \frac{1}{3} \cdot (d-d_s)$$

If $d_s > d$

$$F_{gp} = 0$$

$$M_{F_{gp}} = 0$$

- The forced caused by the weight of the structure:

$$V_c = B \cdot (H+d) \cdot \gamma_c$$

If $d_s < d$

$$M_{V_c} = 0$$

If $d_s > d$

$$M_{V_c} = B \cdot (H + d) \cdot \gamma_c \cdot \frac{1}{2} \cdot (d_s - d)$$

The extent to which the scour hole reaches in horizontal direction underneath the foundation of the structure is assumed to be in the order of magnitude of d_s-d.

- The force caused by the upward hydraulic force underneath the structure. The upward hydraulic pressures are taken to be more or less constant over the width of the wall and equal to the pressures exerted by the water level outside.

$$V_w = \gamma_w \cdot (h + d) \cdot B$$

If $d_s < d$

$$M_{V_w} = 0$$

If $d_s > d$

$$M_{V_c} = \gamma_w \cdot (h + d) \cdot B \cdot \frac{1}{2} \cdot (d_s - d)$$

ΣM is formed by the following components:

$$\Sigma M = M_{Fgp} + M_{Fw} - M_{Fga} - M_{Fgw} - M_{Vc} - M_{Vw}$$

ΣV is formed by the following components:

$$\Sigma V = V_c - V_w$$

In these equations:

B = width of the base of the structure, (m)
H = height of the earth embankment behind the structure (m)
d_s = depth of the scour hole caused by the waves (m)
d = depth of the base of the structure with respect to the elevation of the bottom (m)
h = water level (m)
d = depth of the base of the structure with respect to the elevation of the bottom (m)
γ_w = volumetric weight of the water (kN/m^3)
γ_g = density of the dry soil (kN/m^3)
γ_s = density of the saturated soil (kN/m^3)
γ_c = density of the wall material (kN/m^3)
K_a = coefficient applied to get the horizontal active ground force
K_p = coefficient applied to get the horizontal passive ground force
q = superimposed load (kN/m^2)

2. Sliding: Sliding of the structures takes place when the destabilising horizontal forces are bigger than the stabilising ones. The limit state function is as follows:

$L = \Sigma F_e - \Sigma F_d$

$\Sigma F_e = F_w + F_{gp} + F_r$
$\Sigma F_d = F_{ga} + F_{gw}$

Where F_r is the resistance to slide force, given by:

$F_r = (V_c - V_w) \tan \delta$

Where δ is the angle of friction between the base and the underlying soil.

The probability of failure of the flood defence will be the addition of the probability of failure due to both modes and considering them independent.

Condition grades

The deterioration processes of gravity based structures mainly relate to the material of the structure and hence to the failure modes describing structural failure rather than instability problems. Therefore, the moment on the strength side in the limit state function of the gravity based wall is reduced using a factor resp. 1.0, 0.8, 0.6, 0.4, 0.2

Underlying assumptions

In order to define the moments and vertical forces as described above, implicitly a number of assumptions have been made:

- Assumptions with regard to generic dimensions.
- There are no rules defining how much a scour hole extends horizontally underneath a vertical wall when the depth of the scour hole exceeds the depth of the base of the vertical wall. It is assumed that this horizontal distance is in the order of magnitude of the difference between the scour depth and the depth of the base of the vertical wall.
- In some cases the gravity-based wall is founded on piles. These piles have an extra stabilising effect. The presence of piles has been neglected which in some cases may result in a relatively unstable representation of reality.
- The contribution of the horizontal forces exerted by the waves in coastal environments is assumed to be negligible in comparison to the horizontal forces exerted by the ground and the hydraulic pressures of the water. In a more detail analysis of failure of a structure these forces can be calculated as explained in McConnell, Allsop and Flohr, 1998.
- The contribution of the groundwater level in the earth embankment behind the structure is considered to be saturated.
- After the vertical wall has collapsed the expectation is that part of the earth embankment still remains. Before complete breach takes place this remaining earth embankment must be eroded. This remaining strength is neglected in this approach.

Data requirements

Some deliberations with respect to the data requirements are described below:

- Water level h(m): The same reasoning given for sheet piles walls are valid.
- Wall exposed height H(m): This value is known (deterministic) based on local knowledge or from NFCDD.
- Ground density: average values depending on the ground type can be defined from literature. When this density is unknown, Vrouwenvelder *et al*. (2001) recommends to use the values on Table 11.
- Water density: typical values are 10 kN/m^3 for drinking water and 10.3 kN/m^3 for sea water.
- Height and width of the gravity wall: If a local assumption is made for the height, a conservative estimate of the width and the toe depth of the base can be made as a function of the height. Considering sliding (equilibrium of horizontal forces) and tilting (moments equilibrium around critical point) both characteristics can be estimated. In which F is a safety factors are usually taken as 1.5. In this conservative approach the stabilising force of the water level is not taken into account and the earth embankment behind the vertical wall is assumed to be fully saturated. In the absence of better information, the aim is to derive a relation between the height of the vertical wall and the base which provides a rough indication of the order of magnitude.

3.5 Shingle beaches and dunes

3.5.1 Information availability dependant approach to failure probability

Swell waves as well as storms can pose a threat to shingle beaches. The profile of shingle beaches tends to adjust to the governing water level and wave conditions. Wave attack causes the crest level to increase and the crest to retreat landward. The landward retreat is mainly the result of the wave height; the increase in crest level is mainly influenced by the wave period. The response of the shingle beach is to form a natural flood defence against the sea conditions during storms. However, always some overtopping of the shingle beach occurs. The total volume of water is the combination between the overtopping and the water washing through the porous shingle beach.

The limitations in the ability of the shingle beach to form a natural defence are formed by the volume of shingle available in the cross section. Longshore transport during the storm and more gradually in time causes this cross sectional volume to decrease. Another factor that has an important influence on the shingle volume in the profile is the presence of a compacted core within the shingle beach. Due to a compacted core less shingle volume is available to adjust to severe hydraulic loading conditions and the water washes more easily over the compacted core through the permeable shingle layer. The behaviour of a beach in combination with a vertical wall is more complex and still poorly understood.

If the available information is relatively detailed, the following approach is recommended:

- Establish the minimum shingle beach profile which is desired during extreme loading conditions. This can be based on historical events and the knowledge about overtopping rates during severe loading conditions.
- Calculate the response of the shingle beach under a set of hydraulic conditions according to the parametric model developed by Powell (1990), make sure that the parameters fall within the defined ranges of applicability of the formulae. Shift the calculated profile so that the volume of shingle deposited on the crest corresponds with the displaced volume of shingle.
- Failure corresponds with the probability that the profile given the loading conditions exceeds the minimum desired profile under these conditions. This therefore indicates whether the volume in the shingle beach is sufficient to withstand the hydraulic loading conditions imposed upon it.

At the highest level of risk assessment not enough information is available to calculate the probability of failure as described above. Especially the lack of any kind of qualitative or quantitative information (e.g. whether or not a compacted core is present, and some indication of its magnitude) about the volume of shingle in the profile makes the development of a credible approach difficult.

3.5.2 Limit state function

The failure mode that is considered for shingle beaches is the crest retreat given the hydraulic loading conditions exceeds the width of the shingle beach which leads to breach of the beach. This can also be expressed as follows:

$$P\left(failure\ \ barrier\ \ shingle\ \ beach\right) = P\left(p_c \geq w \middle| L\right)$$

In which p_c is the crest retreat of the shingle beach given the hydraulic loading conditions.

The probability of exceedance of the width of the shingle beach by the crest retreat is represented by the following limit state function:

$$L = w - p_c$$

Where:
w = width of the shingle beach, determined by whether the shingle beach is considered to be narrow or wide and the condition grade of the beach.
p_c = represents the crest retreat and as indicated in the parametric model for shingle beach profile. The crest retreat is calculated using the same equations for p_c and the factor for the effective beach width representing the condition grades.

Given the significant wave height, peak wave period and water level the profile of the shingle beach can be calculated with the parametric model according to

Powell (1990). A simplified representation of this model is presented in the figure below. In the figure the continuous line is the initial profile defined by h_c which is the initial crest level and the slope of 1:7. The dashed line represents the schematisation of the response of the shingle beach which 'hinges' around the intersection between the storm water level and the slope of the original beach profile. This intersection is indicated with (0,0). $h_{c;s}$ and p_c are respectively the vertical and horizontal position of the crest level of the response profile and are represented by the formulae below (from Powell, 1990).

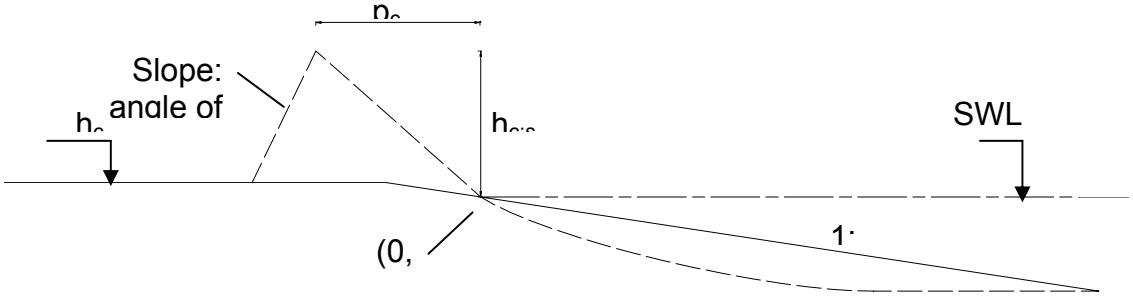

$$h_{c;s} / H_s = 2.86 - 62.69(H_s / L_{om}) + 443.29(H_s / L_{om})^2$$

$$\frac{p_c D_{50}}{H_s L_{om}} = -0.23\left(\frac{H_s T_m g^{1/2}}{D_{50}^{3/2}}\right)^{-0.588}$$

Figure 13 Simplified representation of parametric model according to Powell (1990)

Where
p_c = crest retreat after the storm, with reference to the intersection between the water level and the beach slope, point (0,0).
h_c (m)= crest height
$h_{c,s\ (m)}$= crest height after the storm, with reference to the intersection between the water level and the beach slope, point (0,0)
L_{om} (m) = offshore wave length
H_s (m)= wave significant height
T_m (s)= wave period
D_{50} (m)= material mean size

Range of validity

H_s/L_{om} – 0.01-0.06
$H_sT_mg^{1/2}/D_{50}^{3/2}$ = 3000-55000

1. The simplification of the parametric model replaces the normally applied strategy to determine the total response profile under the loading conditions and shift the profile such that the areas underneath and above the line equal. The chosen simplification is based on experience with shingle beaches, which points out that most of the shingle beach profiles more or less 'hinge' around the water level.

2. Slopes of shingle beaches under relatively calm sea conditions can be linked to the size of the shingle, if for instance three sizes are defined:

Table 15 Definition of beach material sizes

Beach	Slope	Material size (D_{50})
Fine	1:12	10 mm
Medium	1:9	20 mm
Coarse	1:7	40 mm

The crest level under calm sea conditions is given, although this is dependent upon the time at which this level is observed. For the generic fragility curve medium sized shingle was picked.

The condition of the shingle beach depends on the availability of volume in the profile. The limit state function developed above, for use in case of restricted data availability, does not relate to volume considerations. To keep the definition of the condition grade easy to interpret, the strength side in the limit state function of the shingle beach is multiplied with a factor of resp. 1, 0.8, 0.6, 0.4, 0.2

3.6 Dunes

3.6.1 Introduction

Dunes should be approached similarly as shingle beaches: estimating the crest level and crest retreat and then calculating the probability of breaching. Condition grades by including a factor in the crest retreat. During a storm the front face of the dune erodes and the eroded material is deposited on the foreshore of the dune. Breach occurs when the remaining profile is insufficient to withstand storm conditions. The profile of the dune as a function of the loading conditions during storm is predicted with the model according to Vellinga (1986), see figure below.

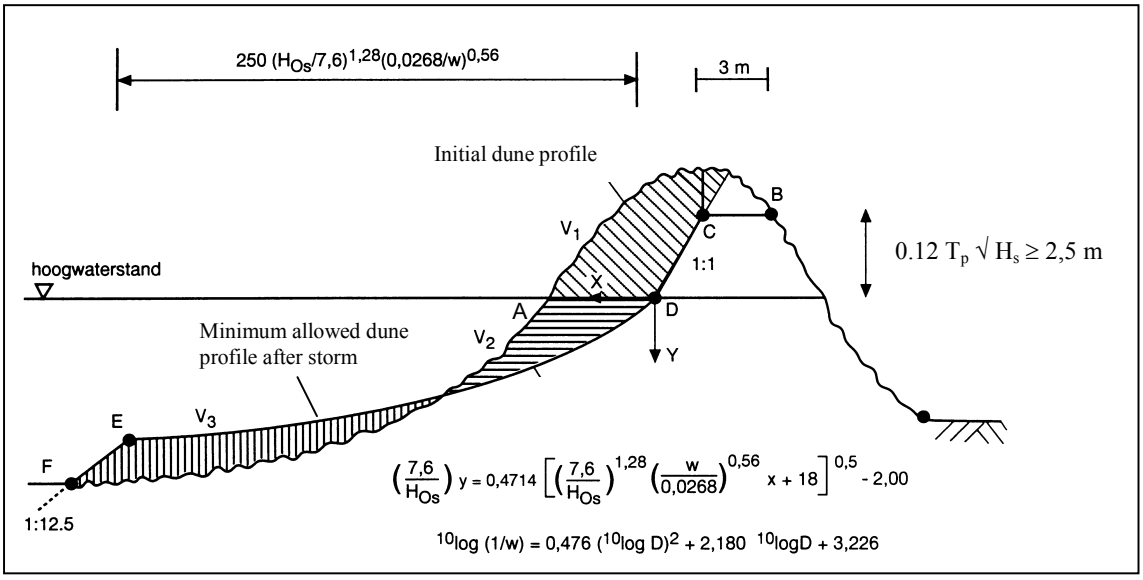

Figure 14 Comparison of the initial profile of the dune and the minimum allowed profile as a result of the storm (from Vrouwenvelder *et al*. (2001))

As explained in the literature review in PC-Ring failure of dunes is approached by comparing the initial profile of the dune and a minimum allowed profile as a result of the storm, see Figure above. The minimum allowed profile under a storm is represented by the line BCDEF, for which the stretch between D and E is determined according to Vellinga (1986), the formula is given in the figure. The limit state function establishes whether the initial profile is sufficient to provide the minimum allowed profile:

$Z = m_D \ V_1 + V_2 - V_3$

In which V_1, V_2 and V_3 are defined according to Figure 14 and m_D is a factor taking the model uncertainty into account.

3.6.2 Approach in case of restricted data availability

The approach as explained in section 3.6.1 requires detailed knowledge about the profile of the dune, which is highly variable. In addition, local expert input is needed on the minimum acceptable profile during a storm to prevent breaching. This section describes a possible approach when data availability is limited to crest level (hc) toe level (tl) and simplified slopes (tan o and tan s), see figure 15.

The limit state function is defined as follows:

$Z = m_R \ dw - m_S \ cr$

In which dw is the width of the dune, and cr is the crest retreat caused by the storm, m_R and m_S are model factors, taking account of the uncertainty involved with the simplified models. In order to estimate the crest retreat during the storm, the response dune profile needs to be determined. A number of

iterations are made whereby the aim is to achieve $V_1+V_2+V_3+V_4 = A_1+A_2+A_3$. See figure 15. The shape of the response profile is determined with the equation in figure 14.

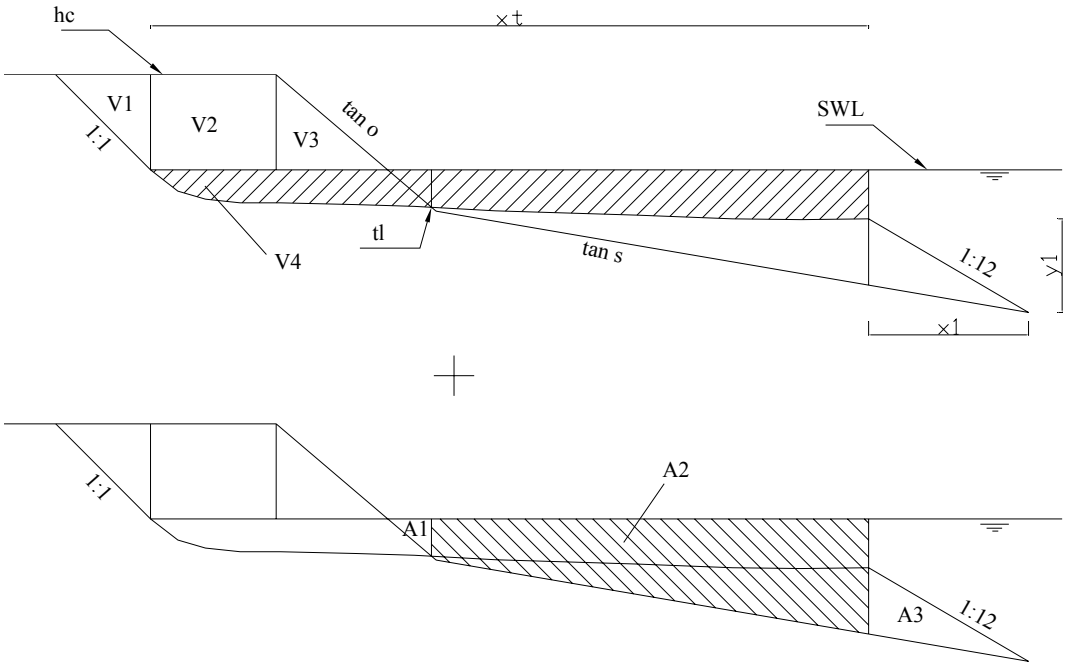

Figure 15 Simplified approach to dunes in case of restricted data availability

The following expressions are used to calculate V_1, V_2, V_3, V_4, A_1, A_2 and A_3.

$$V_1 = \tfrac{1}{2}\left(h_c - h\right)^2$$

$$V_2 = \left(h_c - h\right) d$$

$$V_3 = \frac{\tfrac{1}{2}\left(h_c - h\right)^2}{\tan o}$$

$$V_4 = \left[\frac{H_s}{7.6}\cdot 0.47 \cdot \frac{1}{C_1 \cdot 1.5}\left\{C_1 \cdot x_t + 18\right\}^{1.5} - 2x_t - hx_t\right] - \left[\frac{H_s}{7.6}\cdot 0.47 \cdot \frac{1}{C_1 \cdot 1.5}\cdot 18^{1.5}\right]$$

$$C_1 = \left(\frac{7.6}{H_s}\right)^{1.28}\left(\frac{w}{0.0268}\right)^{0.56}$$

$$A_a = \frac{\tfrac{1}{2}\left(h - tl\right)^2}{\tan o}$$

$$A_2 = \left(x_t - \left(\frac{h - tl}{\tan o} + d\right)\right)\left(h - tl\right) + \tfrac{1}{2}\left(x_t - \left(\frac{h - tl}{\tan o} + d\right)\right)^2 \cdot \tan s$$

$$A_3 = \tfrac{1}{2} x_1 y_1 - \tfrac{1}{2} x_1 \left\{ y_1 - \left(x_t - \left(\frac{h - tl}{\tan o} + d \right) \right) \cdot \tan s \right\}$$

$$x_1 = \frac{\left(x_t - \left(\frac{h - tl}{\tan o} + d \right) \right) \cdot \tan s}{\frac{1}{12} - \tan s}$$

$$y_1 = \tfrac{1}{12} x_1$$

In which h_c is the crest level of the dune, tl is the toe level of the initial dune profile, h is the storm water level, tan o and tan s represent the slope of the initial dune profile in a simplified way, H_s is the significant wave height and w is the fall velocity of the sand particles.

V_4 represents the area between the storm water level and the response profile of the dune. The expression above is derived by taking the primitive function of the equation in figure 14.

For condition grades are reflected by reducing he dune width in the limit state function with factors 1, 0.8, 0.7, 0.6, 0.5.

4. References

British Steel Corporation, (1981). BSC Sections, Piling Handbook. Third Edition 1981

CUR 190, (1997) Kansen in de civiele techniek, deel 1: Probabilistisch ontwerpen in theorie (Chances in civil engineering, part 1: Probabilistic design in theory (in Dutch)), CUR report 190, Gouda

Dekker, R. (1996) Applications of maintenance optimization models: a review and analysis, Reliability and System Safety 51, pp. 229-240

Dekker, R., Scarf, P.A. (1998) On the impact of optimisation models in maintenance decision making: the state of the art, Reliability Engineering and System Safety 60, pp. 111-119

Hall, J.W., Dawson, R.J., Sayers, P.B., Rosu, C., Chatterton, J.B., Deakin, R., (2003). A methodology for national-scale flood risk assessment. Proc. *ICE Water and Maritime Engineering*, Vol.154. Sept. p.235-247.

HR Wallingford, (2004). Risk assessment for flood and coastal defence for strategic planning, A summary. Report W5B-030/TR

McConnell, K., (1998). Revetment systems against wave attack – A design manual, Thomas Telford

McConnell, K.J., Allsop, N.W.H. & Florh, H., (1999). Proceedings of Coastal Structures; Santander , Spain; 7th-10th June 1999, pp447-454.

Powel, K.A., (1990). Predicting short term profile response for shingle beaches, Report SR219, HR Wallingford.

TAW (Technical Advisory Committee for Flood Defence in the Netherlands), (1999). Guidelines on Sea and Land Dikes. The Hague. pp85.

Terzaghi, K, and Peck, R.B. (1967) Soil Mechanics in Engineering Practice. John Wiley & Sons, New York.

Vellinga, P., (1986). Beach and dune erosion during storm surges. Thesis Delft University of Technology, also: Delft Hydraulics, Communications No.372, The Netherlands

Vrouwenvelder, A.C.W.M., Steenbergen, H.M.G.M., Slijkhuis, K.A.H., (2001). Theoretical manual of PC-Ring, Part A: descriptions of failure modes (in Dutch), Nr. 98-CON-R1430, Delft.

Vrouwenvelder, A.C.W.M., Steenbergen, H.M.G.M., Slijkhuis, K.A.H., (2001). Theoretical manual of PC-Ring, Part B: statistical models (in Dutch), Nr. 98-CON-R1431, Delft.

5. List of abbreviations

CG **Condition Grade**

FEMA **Failure Modes and Effects Analysis**

HLM **High Level Method (RASP)**

HLM+ **High Level Method Plus (RASP)**

NaFRA **National Flood Risk Assessment**

NFCDD **National Flood and Coastal Defence Database**

RASP **Risk Assessment of flood and coastal defence for Strategic Planning**

Appendices

Appendix 1 Examples of RASP HLM+ fragility curves

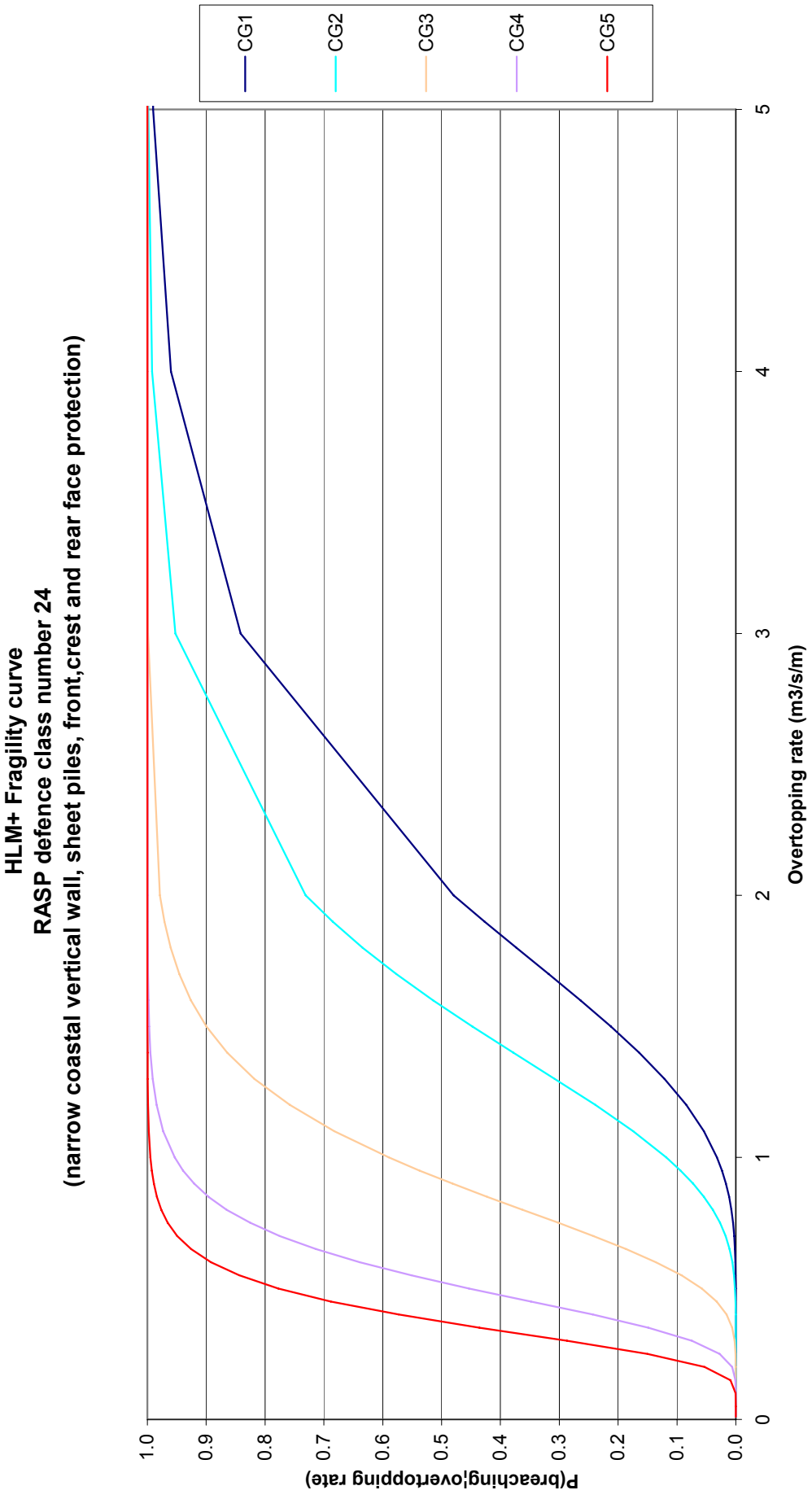
HLM+ Fragility curve
RASP defence class number 24
(narrow coastal vertical wall, sheet piles, front,crest and rear face protection)
CG1
CG2
CG3
CG4
CG5
P(breaching|overtopping rate)
1.0
0.9
0.8
0.7
0.6
0.5
0.4
0.3
0.2
0.1
0.0
0
1
2
3
4
5
Overtopping rate (m3/s/m)

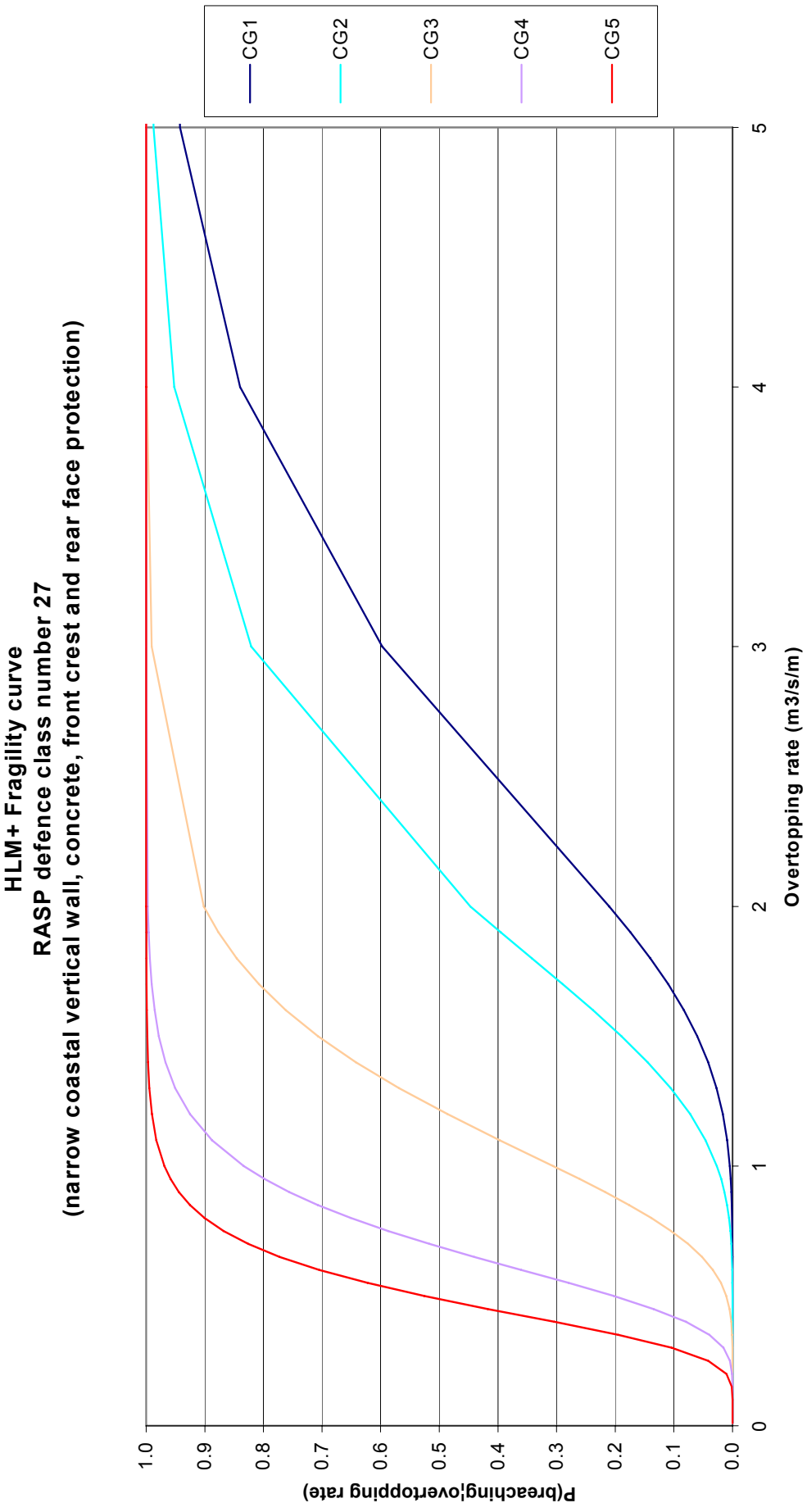
HLM+ Fragility curve
RASP defence class number 27
(narrow coastal vertical wall, concrete, front crest and rear face protection)
CG1
CG2
CG3
CG4
CG5
P(breaching|overtopping rate)
1.0
0.9
0.8
0.7
0.6
0.5
0.4
0.3
0.2
0.1
0.0
0
1
2
3
4
5
Overtopping rate (m3/s/m)

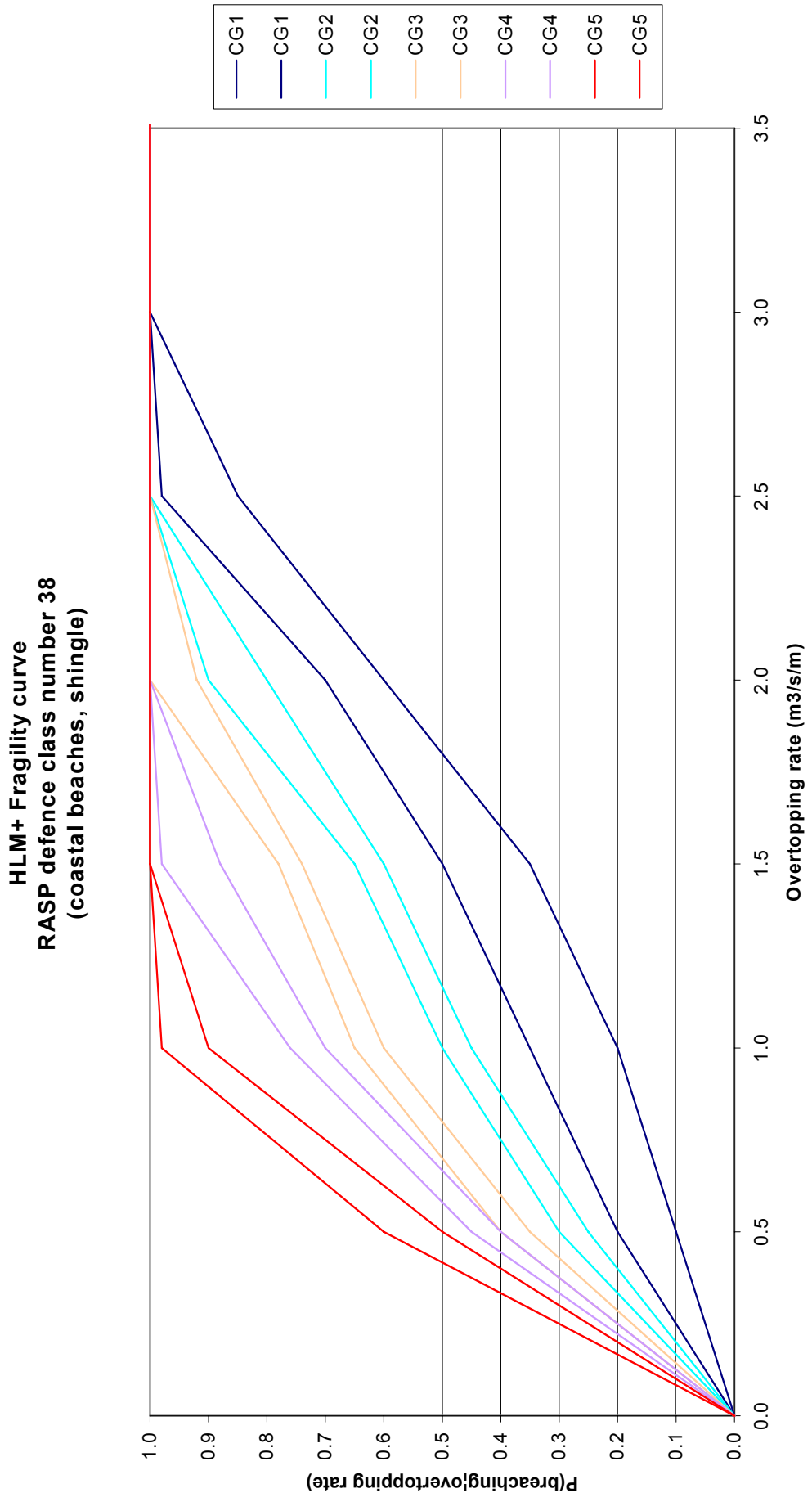
HLM+ Fragility curve
RASP defence class number 38
(coastal beaches, shingle)
CG1
CG1
CG2
CG2
CG3
CG3
CG4
CG4
CG5
CG5
P(breaching|overtopping rate)
1.0
0.9
0.8
0.7
0.6
0.5
0.4
0.3
0.2
0.1
0.0
0.0
0.5
1.0
1.5
2.0
2.5
3.0
3.5
Overtopping rate (m3/s/m)

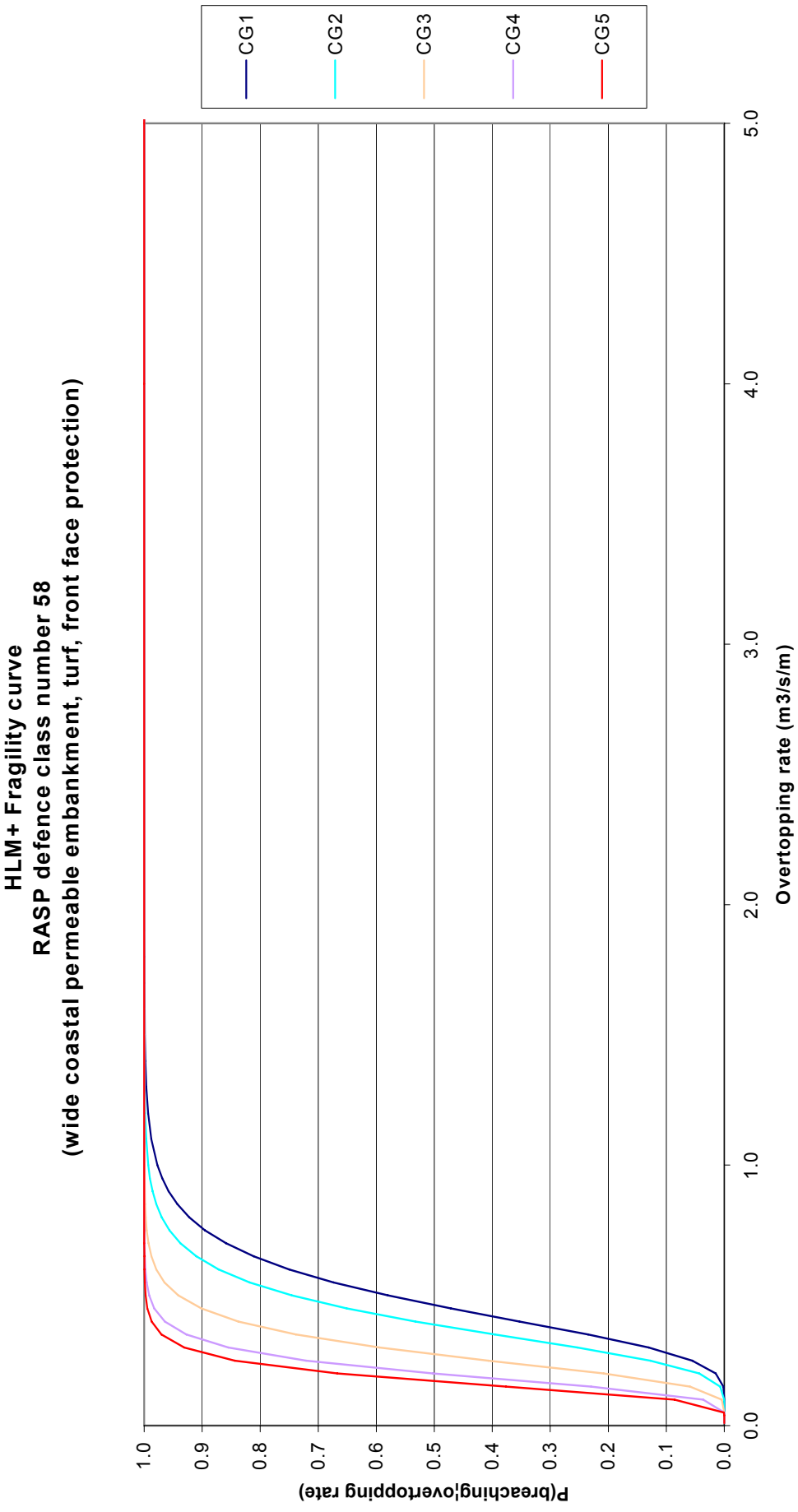
HLM+ Fragility curve
RASP defence class number 58
(wide coastal permeable embankment, turf, front face protection)
CG1
CG2
CG3
CG4
CG5
P(breaching|overtopping rate)
1.0
0.9
0.8
0.7
0.6
0.5
0.4
0.3
0.2
0.1
0.0
0.0
1.0
2.0
3.0
4.0
5.0
Overtopping rate (m3/s/m)

Appendix 2 More advanced Generic fragility curves

Appendix 3 Probabilistic Methods

The ‘Guidelines for Environmental Risk Assessment and Management’ is used as the basic guidance in the UK to assess and manage environmental risk. The main framework for risk assessment advised in these guidelines is shown in Figure 1. According to this framework risk assessments are performed at three tiered levels and the risk assessment of each tier consists of the same procedure.

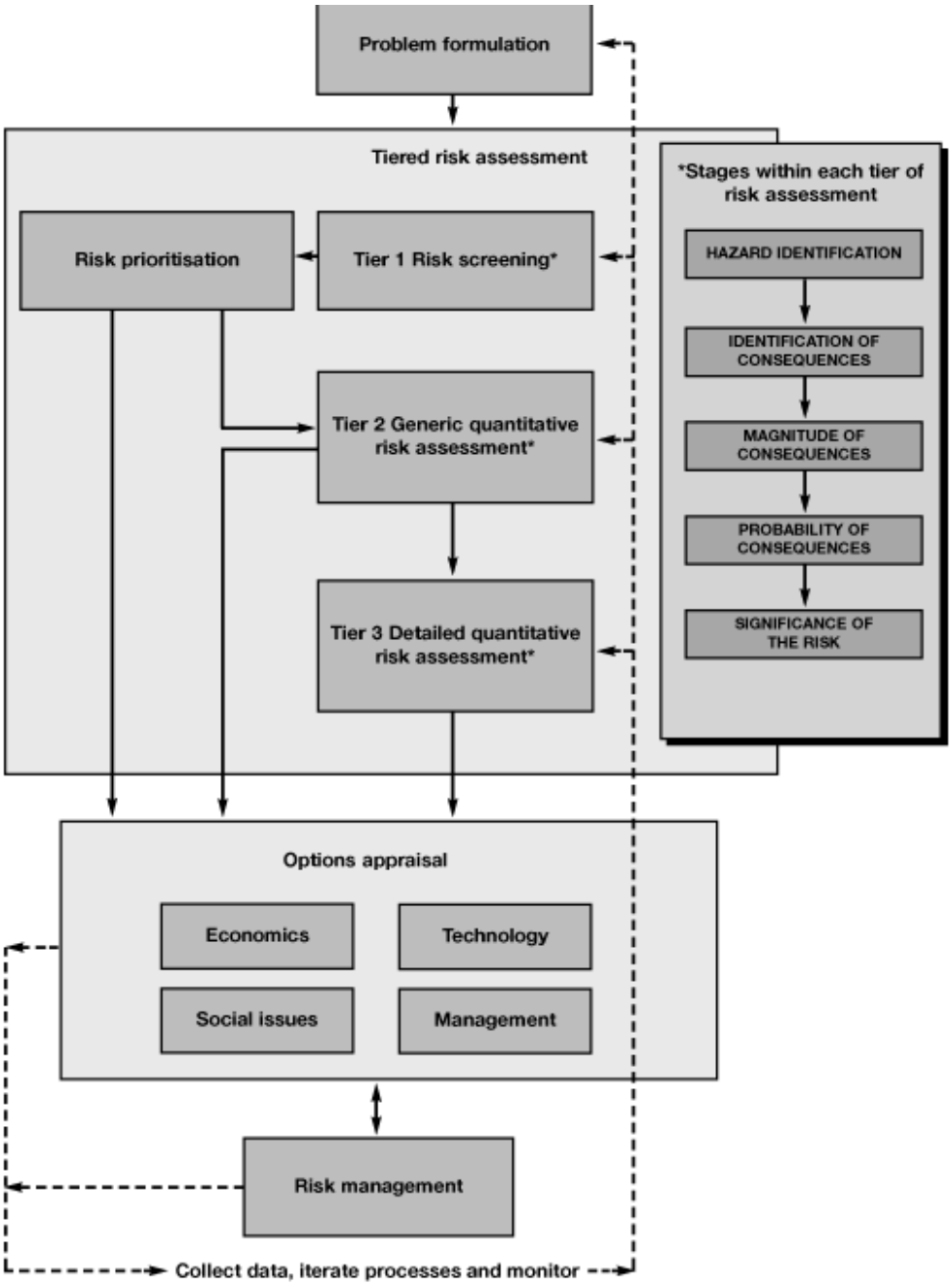

Figure 1 Framework for environmental risk assessment and management (from ‘Guidelines for Environmental Risk Assessment and Management’ by the DEFRA)

1. Risk assessments and the position of reliability analysis herein

Below first the steps that must be taken in each tier of risk assessment are mentioned and the role of the reliability analysis herein will be discussed.

1.1. Risk analysis in a general sense

Risk is a function of the probability of undesired events and their consequences. A risk assessment is divided in the following steps, see Figure D.1., see the original guidelines for more detail:

- *Hazard identification*, in case of flood and coastal defences this amounts to for instance a tidal surge
- *Identification of the potential consequences* that might arise from a hazard
- The *magnitude of the consequences*, part of this is to address the spatial scale, the temporal scale and the time to onset of the consequences
- *The probability of the consequences* which can be divided into: the probability of the hazard occurring, the probability of the receptors being exposed to the hazard, the probability of harm resulting from exposure to the hazard
- *The significance of risk*, relating the risk to for instance acceptable risk levels.

1.2. Reliability analysis

Considering the steps in the risk assessment as mentioned in D.1.1., the reliability analysis is the part in risk assessments that deals with the qualitative and quantitative aspects of the probability of the hazard occurring and the probability that the receptors are being exposed to the hazard. Related to coastal and flood defences this amounts to the probability of breach occurring at one or more places along the flood and coastal defence system. Below the text will specify reliability of an element and of a system in terms of definitions.

Reliability of an element
According to [CUR 190] the reliability of an element is defined as follows below. A **limit state** is the state when failure is nearly occurring. The **reliability** is the probability that this limit state will not be exceeded. The general appearance of a limit state function is:

$$Z = R - S$$

In which R is the “strength” (resistance) or: the resistance against failure; S is the “loading” (solicitation) or: that which induces failure.

The limit state is described by Z = 0 and the probability of failure is:

$$P_f = P(Z \leq 0) = P(S \geq R)$$

The reliability is the probability P(Z>0) and is the complement of the probability of failure:

$$P(Z > 0) = 1 - P_f$$

The point in the failure space with the biggest probability density is called the design point. Usually this point is located on the border between safe and unsafe area.. The design point plays an important role for several techniques when determining the probability of failure.

The calculation of the probability of failure using Z = R-S is called a structural reliability analysis. A **failure mode** is the way in which an element fails. The mentioned Z-function represents one failure mode.

Reliability of a system
According to [CUR 190] **a system** can be defined as: an assembly of elements or processes with a common purpose. A system can be formed by a configuration of physical components or processes, but also by a number of failure modes or a combination of failure modes and a configuration of components.

The **reliability of a system** is the extent to which the system fulfils its requirements. Based on the foregoing it can be said that the reliability of the system is determined by the reliability of its elements and the relations between the elements. If the system cannot fulfil its requirements, the system fails.

1.3. Methods of system analysis

Below a number of methods that are applied to analyse systems are mentioned, [CUR 190].

FMEA (= Failure modes and effects analysis) is a risk analysis which is based on the following schematic approach:

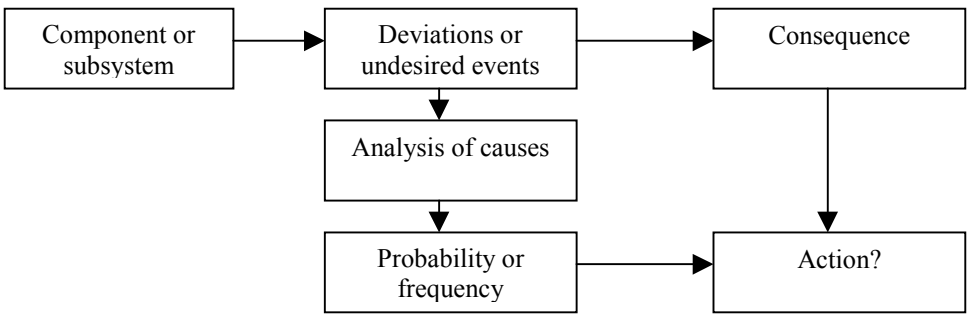

Figure 2 FMEA schematic approach (From CUR 190)

The main purpose of a FMEA is to give an as detailed view as possible of all the foreseen undesired events and consequences in a system or process, so that can be argued which actions should be undertaken.

- *FMECA (= Failure modes, effects and criticality matrix)* is a FMEA with an additional criticality matrix. In this matrix the different failure modes and consequences are related and the consequences are ranked based on the severity of the consequence

- *Tree of events* is an aid of an analysis of the response of a system to one event. The tree of events relates on a logical way one ‘start event’ and all possible consequences by inventorying and analysing all possible events that can follow the ‘start event’
- *Fault tree* lists the logical succession of all events that lead to one undesired top event. This event is placed in top of the tree. Fault trees are especially suitable for displaying cause-consequence chains that lead to an undesired top event when one cause has two distinct consequences (yes or no, positive or negative, good or bad, failing or not failing, etc.). Only the negative consequences are listed in the fault tree
- *Cause consequence chart* is a combination between the tree of events and the fault tree. This combination is made because of the following reason: both the tree of events and the fault tree have as a disadvantage that the consequences of the failure of an element or subsystem in an overall good functioning total system are not made visible. For the display of consequences that cannot be very easily differentiated the cause-consequence chart is more suitable.

2. Methods for quantitative reliability analyses

The calculation methods of the probability of failure based on the limit state function can be grouped into the following main categories:

i) Fundamental solution based on integrating the joint probability density function of the variables in the limit state function over the area which is connected to failure, i.e. the area for which the limit state function is negative
ii) Methods which are based on transforming the variables of the limit state function into standard normal variables and iteratively linearising the limit state function in different points until the design point has been found. The design point is defined as the point on the limit state function with the highest probability density and therefore reflects the highest probability of Z taking the value of zero
iii) Semi-probabilistic methods using the values of variables which in case of loading have a probability 95% being not exceeded and in case of strength have a probability of 95% being exceeded. The strength values are therefore conservatively low and the loading values are conservatively high
iv) Deterministic approach based on average values of the variables and using a safety factor to cover the uncertainty.

2.1. Level III Calculations

The background of level III calculations is lined out below. The probability of failure is defined according to equation (1) given below. It amounts to integrating the joint probabilities of the combinations of strength and loading for which the limit state function is negative. In other words, the probability of failure is calculated by integrating (1) for those combinations for which the strength is smaller than the loading.

$$P(Z<0)=\iint_{Z<0} f_{R,S}(R,S)\,dR\,dS \tag{1}$$

where:

$P(Z<0)$ - probability of failure

$f_{R,S}(R,S)$ - joint probability density function of strength, *R,* and loading, *S*

As it is in most cases impossible to find an analytical solution for this integral numerical methods are applied to make approximations. Examples are the Riemann procedure or Importance Sampling and the Monte Carlo method.

Monte Carlo simulation

The information below is taken from CUR (1997). The joint probability distribution function of the variables in the limit state function can be written as:

$$F_{\vec{X}}(\vec{X}) = F_{X_1}(X_1)F_{X_2|X_1}(X_2|X_1)\cdots F_{X_m|X_1,X_2,..,X_{m-1}}(X_m|X_1,X_2,\ldots,X_{m-1}) \tag{2}$$

A distribution function F_{Xi} take values in an interval between 0 and 1. These values are uniformly distributed between 0 and 1. The Monte Carlo method draws m values, X_{U_1} to X_{U_m} , from a uniform distribution function taking values between 0 and 1 and transforms them as follows:

$$\begin{aligned} X_1 &= F_{X_1}^{-1}(X_{U_1}) \\ X_2 &= F_{X_2|X_1}^{-1}(X_{U_2|X_1}) \\ &\vdots \\ X_m &= F_{X_m|X_1,X_2,..,X_{m-1}}^{-1}(X_{U_m}|X_1,X_2,\ldots,X_{m-1}) \end{aligned} \tag{3}$$

In case of independent variables this works out as:

$$X_i = F_{X_i}^{-1}(X_{U_i}) \tag{4}$$

These transformations result in a value for each variable in the limit state function. These values can then be implemented in the limit state function to find out whether for this combination the function is smaller or larger than 0. This procedure is run a large number of times and the probability of failure is calculated by:

$$P_f \approx \frac{n_f}{n}$$

In which n_f is the number of times for which a negative value is calculated for the limit state function and n is the total number of simulations.

A way to determine the design point is by calculating the probability density of each combination of variables and holding on to the combination of variables with the highest joint density.

According to Vrijling (2000) the Monte Carlo simulation method is especially suitable when the limit state function is relatively simple and the probability of failure is not too small. In most cases, however, it is advised to determine the probability of failure by a level II approach.

2.2. Level II Calculations

The FORM (=First Order Reliability Method) is demonstrated using an example based on a linear limit state function with independent, normally distributed variables. Secondly, approximations for the non-linear case are shown.

Linear limit state function
The calculation of the probability of failure of a linear limit state function with normally distributed independent variables is quite straightforward. However, the simple case demonstrates the definitions that form the basis of non-linear limit state functions with possible dependent not normally distributed variables. The following steps are taken:

- Introduction normal and standard normal density functions
- Transformations from normal to standard normal space
- The relation between the probability of failure and the reliability index, β
- The graphical representation of the reliability index β
- Implications for more complex limit state functions.

The limit state function is for now considered to be linear and to have independent, normally distributed components:

$$Z = R - S \tag{5}$$

Normal and standard normal density functions
The normally distributed variables have the following probability density function:

$$f_X(X) = \frac{1}{\sqrt{2\pi}\sigma_X} \exp\left(- \frac{(X-\mu_X)^2}{2\sigma_X^2} \right)$$

The standard normal distribution is equal to the normal distribution with mean μ = 0 and standard deviation σ = 1. In other words:

$$f_{U_X}(U_X) = \frac{1}{\sqrt{2\pi}\sigma_X} \exp\left(- \frac{(U_X)^2}{2} \right)$$

Transformations between normal and standard normal distributed variables.

Transformations between normal distributed variables and standard normal distributed variables is done as follows:

$$U_i = \frac{X_i - \mu_X}{\sigma_X} \text{ or } X_i = U_i \sigma_X + \mu_X \tag{6}$$

Transformation of the components of the limit state function Z to standard normal distributed variables amounts to

$$Z = (\mu_R + \sigma_R U_R) - (\mu_S + \sigma_S U_S) = \mu_R + \sigma_R U_R - \mu_S - \sigma_S U_S = 0$$
$$U_S = \frac{\mu_R - \mu_S}{\sigma_S} + \frac{\sigma_R}{\sigma_S} U_R \tag{7a & 7b}$$

See Figure B.1. for a graphical representation of this linear limit state function.

Probability of failure and reliability index
The probability of failure corresponds with the probability that Z is smaller than 0 and is found by transforming Z to the standard normal distribution.

$$P(Z<0)=\Phi\left(\frac{0-\mu_Z}{\sigma_Z}\right)=\Phi\left(-\frac{\mu_Z}{\sigma_Z}\right)=\Phi(-\beta) \tag{8}$$

In which β represents the reliability index and plays a central role in level II calculations. In case of a linear limit state function with independent normally distributed variables μ_Z and σ_Z are easy to derive as follows:

$\mu_Z = \mu_R - \mu_S$

$$\sigma_Z=\sqrt{\sigma_R^2+\sigma_S^2}$$

However, in the standard normal space β has an additional meaning which is explained below.

Graphical representation of β
As can be seen in Figure 3, β is the length of the line which starts in the origin and connects perpendicular to the line represented by the limit state function. This line is also the shortest distance between the limit state function and the origin. How the length of β is derived is shown below. This is the definition according to Hasofer and Lind

$$\cos a=\frac{\sigma_S}{\sqrt{\sigma_R^2+\sigma_S^2}}=\frac{\beta\sigma_S}{\mu_R-\mu_S} \rightarrow \qquad \beta=\frac{\mu_{R-}\mu_S}{\sqrt{\sigma_R^2+\sigma_S^2}}=\frac{\mu_Z}{\sigma_Z}$$

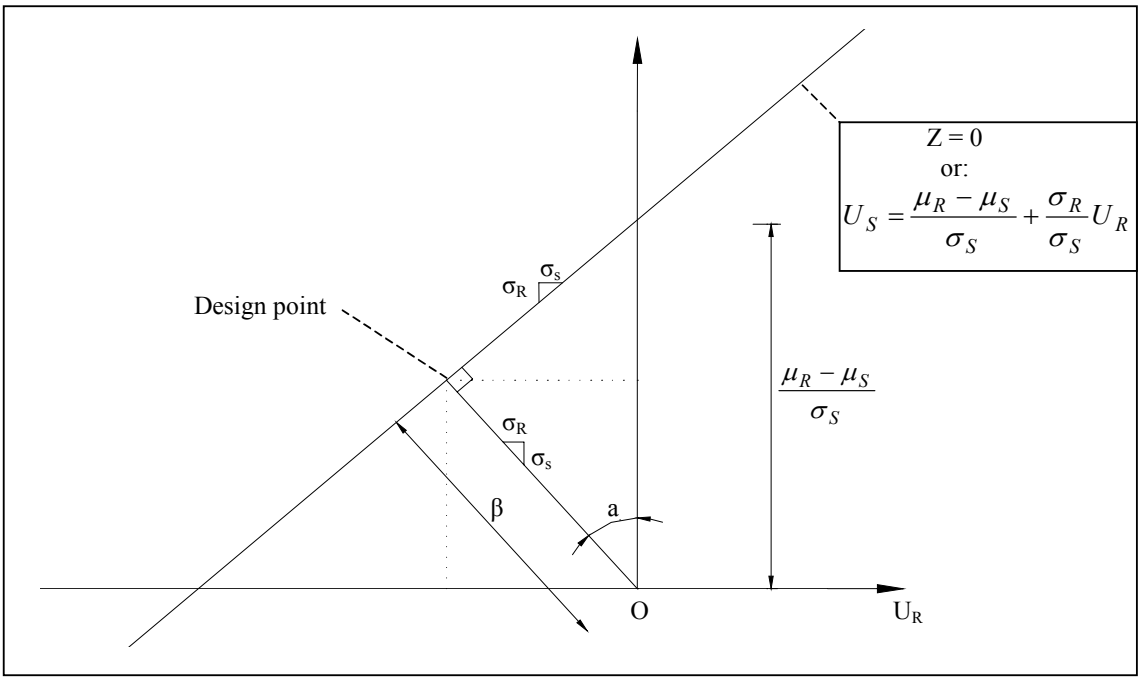

Figure 3 Limit state function as a function of standard normal distributed variables U_R and U_S

The coordinates of the design point are:

$$U_{R;d} = \sin(a) * \beta = \frac{\sigma_R}{\sqrt{\sigma_R^2 + \sigma_S^2}} \beta = \frac{\sigma_R}{\sigma_Z} \beta = \alpha_R \beta \quad (9a)$$

$$U_{S;d} = \cos(a) * \beta = \frac{\sigma_S}{\sqrt{\sigma_R^2 + \sigma_S^2}} \beta = \frac{\sigma_S}{\sigma_Z} \beta = \alpha_S \beta \quad (9b)$$

Other notation of limit state function

An other notation of the limit state function in the Design Point is as shown below.

$$Z_{lin} = B + A_1 u_1 + A_2 u_2 + \ldots \quad (10)$$

Keeping in mind that u_i is a standard normal variable with mean $\mu_{ui} = 0$ and standard deviation $\sigma_{ui} = 1$, the following properties can be derived for Z_{lin} :

$$\mu_{Z\,lin} = B + \sum_{i=1}^{n} \mu_{u_i} = B \quad (11)$$

$$\sigma_{Z\,lin} = \sqrt{\sum_{i=1}^{n} \left(A_i\, \sigma_{u_i}\right)^2} = \sqrt{\sum_{i=1}^{n} A_i^2} \quad (12)$$

$$\beta = \frac{B}{\sqrt{\sum_{i=1}^{n} A_i^2}} \quad (13)$$

Dividing all the components in equation (10) by $\sqrt{\left(\sum_{i=1}^{n} A_i^2\right)}$ results in (14)

$$Z_{lin} = \beta + \alpha_1 u_1 + \alpha_2 u_2 + \ldots \quad (14)$$

where:

α_i - factor of influence of variable X_i

$$\alpha_i = \frac{A_i}{\sqrt{\sum_{i=1}^{n} A_i^2}} \quad (15)$$

Implications for more complex limit state functions

The following implications for more complex limit state functions, i.e., non-linear, not normally distributed and/or dependent variables are based on the above described graphical representation:

- The reliability index β represents the probability of failure in the standard normal distribution. β is the shortest distance between the origin and the limit state function.
- The coordinates of the design point are defined by ($\alpha_R\beta$, $\alpha_S\beta$), in which α_R represents the contribution of the uncertainty of the strength variable to the total uncertainty of the limit state function. α_S represents the contribution of the uncertainty of the loading variable to the total uncertainty of the limit state function.
- The complex limit state function should be worked into a linear case by using Taylor linearisation in the design point. The not normally distributed and/or dependent variables should be transformed into standard normal distributed and independent variables in the design point by using respectively the Rackwitz-Fiessler transformation, see Rackwitz (1977) or Vrijling (2000), and the Rosenblatt transformation (CUR (1997)).
- As the design point is not known beforehand, the calculations are an iterative process.

Non-linear limit state function
If the limit state function is non-linear, a Taylor approximation can be used to linearise the limit state function in the design point. Iterations can then be carried out to find the value of the design point. This design point corresponds with the shortest distance between the origin in the standard normal space and the limit state function.

Two paths can be chosen. Either first convert the limit state function to the standard normal variables and then linearise and continue to do the iterations, or linearise the limit state function, define the design point in normal variables and then continue to do the iterations. The second approach is more practical to implement in computer programming and is therefore chosen to describe in more detail.

Taylor approximation of Z

$$Z = f\left(\vec{X}\right) \approx f\left(\vec{X}^*\right) + \sum_{i=1}^{n}\left(\frac{\partial f\left(\vec{X}^*\right)}{\partial X_i}\right)\cdot\left(X_i - X_i^*\right) \tag{16}$$

In which $\vec{X}^*$ are the co-ordinates of the design point and therefore:

$$\mu_Z \approx f\left(\vec{X}^*\right) + \sum_{i=1}^{n}\left(\frac{\partial f\left(\vec{X}^*\right)}{\partial X_i}\right)\cdot\left(\mu_{X_i} - X_i^*\right) \tag{17}$$

$$\sigma_Z \approx \sqrt{\sum_{i=1}^{n}\left(\frac{\partial f\left(\vec{X}^*\right)}{\partial X_i}\cdot\sigma_{X_i}\right)^2} \tag{18}$$

Remember:

If X is a random variable with:

$E(X) = \mu_X$

$Var(X) = \sigma_X^2$

Then for Y = aX+b

$E(Y) = a\,\mu_X + b$

$Var\,(Y) = a^2\sigma_X^2$

Set of equations for iterations

The set of equations that can be used in practice to make the calculations is:

$$\alpha_i = \frac{\frac{\partial f\left(\vec{X}^*\right)}{\partial X_i}\sigma_{X_i}}{\sigma_Z} \tag{19}$$

$$X_i^* = \mu_i + U_i^*\sigma_{X_i} = \mu_i + \alpha_i\beta\sigma_{X_i} \tag{20}$$

In which α_i represents the factor of influence derived from the Taylor approximation of the limit state function and X_i^* is the value of X_i in the design point. As the design point is unknown beforehand the first step in the iteration is to take a starting value for $\vec{X}^*$ and calculate the new value according to (19) and (20). The iterations continue until a sufficient accuracy is reached.

Non-normally distributed variables

In order to approximate non-normally distributed variables in the normally distributed space, a Rackwitz-Fiessler transformation is applied. How this is done is described below.

Background

Non-normally distributed variables are transformed to normally distributed variables in the design point:

$$F_X\left(X^*\right) = \Phi\left(U^*\right)$$

And therefore:

$$U^* = \Phi^{-1}\left(F_X\left(X^*\right)\right)$$
$$X^* = F_X^{-1}\left(\Phi\left(U^*\right)\right)$$

In which Φ^{-1} is the inverse function of the standard normal distribution and F^{-1} is the inverse function of the non-normally distributed variable.

Keeping this in mind, Rackwitz and Fiessler propose to assume that the values of the non-normal distribution and density functions are equal to those of the standard normal distribution and density functions. This leads to the following set of equations:

$$F_X\left(X^*\right) = \Phi\left(\frac{X^* - \mu_X^{'}}{\sigma_X^{'}}\right)$$

$$f_X\left(X^*\right) = \frac{1}{\sigma_X^{'}}\varphi\left(\frac{X^* - \mu_X^{'}}{\sigma_X^{'}}\right)$$

This leads to values for the mean value and standard deviation of the standard normal distributed variables which substitute the non-normally distributed variables.

Approximating mean value and standard deviation

The mean value and standard deviation of the standard normal distributed variables which substitute the non-normally distributed variables are as follows:

$$\sigma_X^{'} = \frac{\varphi\left(\Phi^{-1}\left(F_X\left(X^*\right)\right)\right)}{f_X\left(X^*\right)}$$

$$\mu_X^{'} = X^* - \Phi^{-1}\left(F_X\left(X^*\right)\right)\sigma_X^{'}$$